Master's degree program in

ENVIRONMENTAL AND TERRITORIAL ENGINEERING

MASTER THESIS

EVALUATING THE EFFICACY OF URBAN HEAT ISLAND MITIGATION STRATEGIES USING OPEN-SOURCE DATA AND ASSESSING THEIR ENVIRONMENTAL IMPACTS IN TEHRAN

Supervisor: Candidate:

Prof. Dabove Paolo Yaghoobian Hirad

Co-Supervisor:

Dr. Bagheri Milad

A.A. 2024/2025

Abstract

In the long term, the rapid expansion of urban zones, especially in megacities, has given rise to several recurring natural challenges. One of the most notable impacts is the Urban Heat Island (UHI) effect, which not only influences the local climate but also contributes to a range of related urban and environmental issues.

This thesis aims to check the Urban Heat Island (UHI) phenomenon, an important natural problem in expanded and big urban districts, with the help of analyzing spatial and temporal patterns and suggesting potential points for mitigation within Tehran's megacity. Rapid progress, plus an increase in the use of resources, caused urban areas to experience warmer temperatures compared to rural surrounding areas in many regions, which may lead to worse environmental, overall public health, and ecological risks. This study gives a total review of the literature on Urban Heat Islands (UHIs) and uses Geographic Information Systems (GIS) with the combination of extra detection methods to check the spatial and temporal changes of UHIs in Tehran. Using data from different satellite images like Landsat 8, MODIS, and Sentinel-2, then based on which data is more convenient for investigation, employs indicators such as the Normalized Difference Vegetation Index (NDVI) and Land Surface Temperature (LST) to check the differences in urban land covers and their impacts on the Urban Heat Island (UHI) effects. Throughout these paths and methods, this research will recognize the hotspot of Tehran city, and suggest the most vulnerable zones, based on checking the land surface and cover, elevation, and population density, that may affect the Urban Heat Island (UHI) intensity. It also assesses the suitable zones for mitigation strategies by emphasizing green-based strategies measurements.

This will be gained with the help of enhancing our understanding of the behavior of UHI patterns in an arid-to-semi-arid megacity like Tehran to help policymakers and city planners. With the help of these investigations and methodologies, natural resilience when urban development increases may be supported, and climate change can be controlled. The aerial measurements and analyses conducted in this research in Tehran address one of the few considerations in this area, with limited comparative inquiries already undertaken.

Keywords: Urban Heat Island (UHI), Land Surface Temperature (LST), Normalized Difference Vegetation Index (NDVI), Urban Greening, Remote Sensing, Tehran, Spatial Analysis, Climate Adaptation.

Acknowledgments

I am deeply grateful to my supervisor, Professor Paolo Dabove at the Polytechnic University of Turin, for his exceptional guidance, unwavering support, and boundless enthusiasm throughout my master's studies and the development of this thesis. His expertise in urban heat island decision-making has greatly enriched my research. I also wish to thank my co-supervisor, Dr. Milad Bagheri, for his valuable advice and encouragement.

Special thanks to the Department of Environmental, Territorial, and Infrastructure Engineering (DIATI) for providing me with the opportunities that have broadened my horizons across climate-related fields and inspired my commitment to protecting our planet.

I am also deeply grateful to my family and my friends for their commitment, support, and faith in me. Their encouragement has been a powerful source of motivation and inspiration throughout my academic adventure.

TABLE OF CONTENTS

Contents

List of Tables

List of Figures

List of Abbreviations

BT	Brightness Temperature
ESA	European Space Agency
GIS	Geographic Information Systems
LSE	Land Surface Emissivity
LST	Land Surface Temperature
MODIS	Moderate Resolution Imaging Spectroradiometer
NDVI	Normalized Difference Vegetation Index
NIR	Near-Infrared
OLI	Operational Land Imager
PV	Proportion of Vegetation
QGIS	Quantum Geographic Information System
ROI	Region of Interest
SWIR	Short-Wave Infrared
TIRS	Thermal Infrared Sensor
TOA	Top of Atmospheric Spectral Radiance
UHI	Urban Heat Island
USGS	United States Geological Survey

List of Equations

1. Introduction

1.1. Definition of Urban Heat Island

Urbanization has advanced to the point where more than 50% of the world's population now resides in urban centers, even though these areas cover only about 2% of the Earth's surface (Un-Habitat, 2008). The United Nations (2007) projects that by 2050, the global population will grow by approximately 2.5 billion, from 6.7 to 9.2 billion, with most of this increase concentrated in urban areas within developing countries. Urban environments are marked by high population densities, extensive infrastructure, elevated energy consumption, and scarce green spaces (Busato et al., 2014), which impose increasing pressure on natural and constructed ecosystems(Roth, 2009). Moreover, this rapid urbanization has led to alterations in the surface characteristics of cities, affecting their radioactive, thermal, moisture, and aerodynamic properties (Kolokotroni & Giridharan, 2008). Notably, the concentration of buildings, roads, and related infrastructure contributes to higher temperatures in urban areas compared to the surrounding rural regions. This temperature disparity is a widely recognized example of anthropogenic climate alteration, commonly called the urban heat island (UHI) (Figure 1).

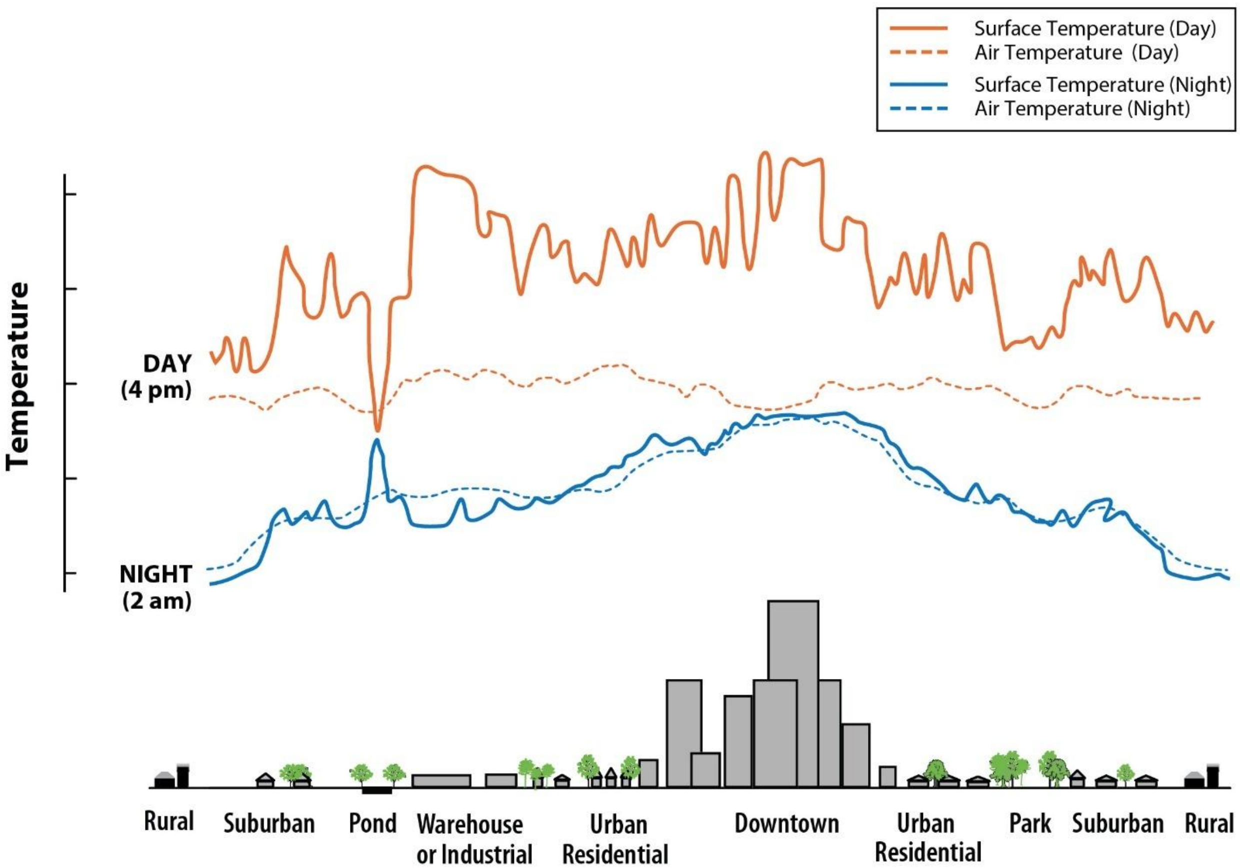

Figure 1. The thermal distribution across various regions is associated with the development of the Urban Heat Island (UHI)(Almeida et al., 2021).

Luke Howard first proposed the concept of the urban heat island (UHI) effect in the early 19th century. By analysing the city of London and its surrounding areas, he examined the impact of urbanization and the factors contributing to the phenomenon (Howard, 1833).

In 1982, Oke showed that the difference in land surface effect was very minor on temperature patterns, vice versa, unexpected changes in temperature from rural to urban land uses, where city centers experienced warmer conditions rather than fringe green zones. This kind of warming can be due to unfiltered pavements, such as buildings and roads, absorbing solar irradiation during the day and re-emitting it as sensible heat, increasing air temperatures, and leading to the urban heat islands (UHI) phenomenon (Oke, 1982).

1.2. The Effects of UHI on the Environment and Human Beings

The urban heat islands (UHIs) phenomenon can lead to a number of socio-economic and environmental challenges, which predict that it may become more serious in the face of global climate change in the future (Corburn, 2007). When the temperature of urban areas increased, it led to an increase in energy consumption demand, which caused strain on the electrical infrastructure, especially during summer and peak usage periods. This increase in the demand for consumption also brings more significant carbon dioxide emissions, which may amplify the effects of climate change. The U.S. Environmental Protection Agency published data that shows that for every 0.6°C rise in temperature in summer, peak electricity demand in urban zones increased by around 1.5% to 2%. The figure below illustrates that the usage of energy increases dramatically when the ambient temperature exceeds the 20–25°C range. The more the dependence on air conditioning stuff, the more human-made heat emissions, which perhaps lead to an increase in local urban area temperatures as well. (Sailor, 2002).

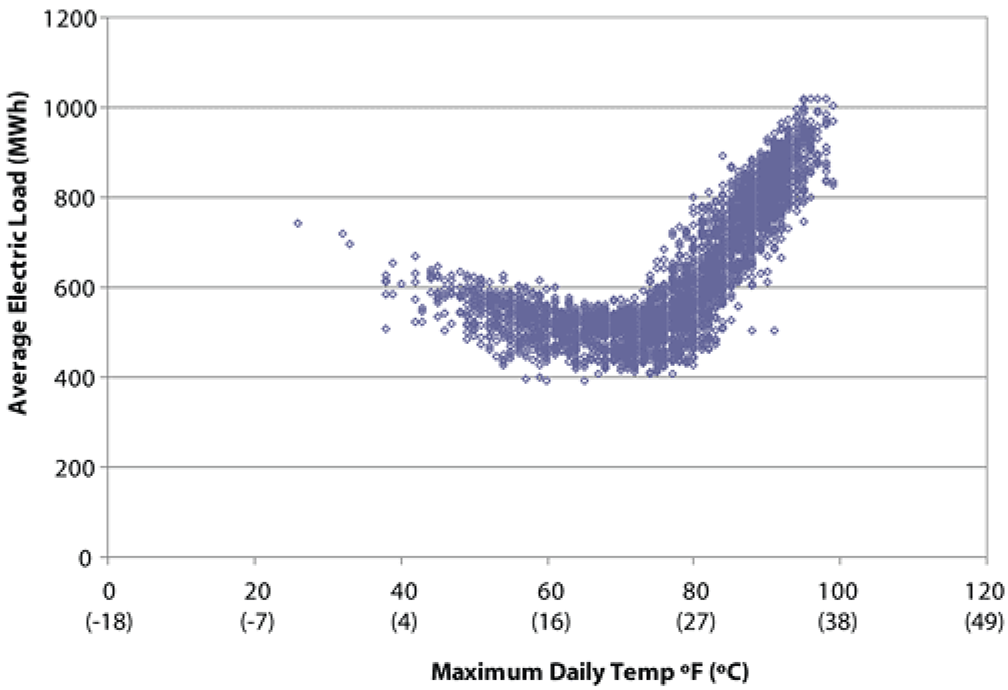

Figure 2. Relationship Between Rising Temperatures and Energy Demand in New Orleans

Furthermore, the meteorological conditions typical of urban heat islands are closely associated with increased air pollution. Elevated temperatures enhance the rate of photochemical reactions, thereby intensifying the formation of ozone and smog. At the same time, reduced wind speeds limit atmospheric dispersion, accumulating heat and pollutants within urban environments (Fallmann et al., 2016). Rising temperatures also tend to elevate water demand, potentially placing pressure on local water supplies and contributing to soil drying. Additional ecological consequences include the earlier onset of plant blooming, exacerbating allergic reactions in sensitive individuals—and an increase in the reproduction rates of insect pests (Fallmann et al., 2016).

High temperatures during the day or even during the night may lead to heat-related illness or even affect public health and mortality. For a long time, exposure to harsh heat has been associated with higher chances of breathing problems, feeling very tired, muscle cramps, stress on the body, heatstroke, organ damage, and more deaths because of extreme heat. These kinds of connections are illustrated in the picture below, which shows the relationship between extreme heat and death risk (Figure 3). In a normal summer weather situation, there is a normal condition of temperature and mortality (section A in the figure). But, when it comes to even a very low increase in the temperature, more than 30°C (86°F) during a hot summer day in today's climate, it can turn to a higher possibility of health risk (UHI impact during heat waves, Part B). However, if this increase in temperature is based on UHI impacts with urbanization and climate change, more extreme heat waves, the consequence may be a higher level of public health risk or even mortality (size of C in Figure 3).(Druckenmiller, 2023).

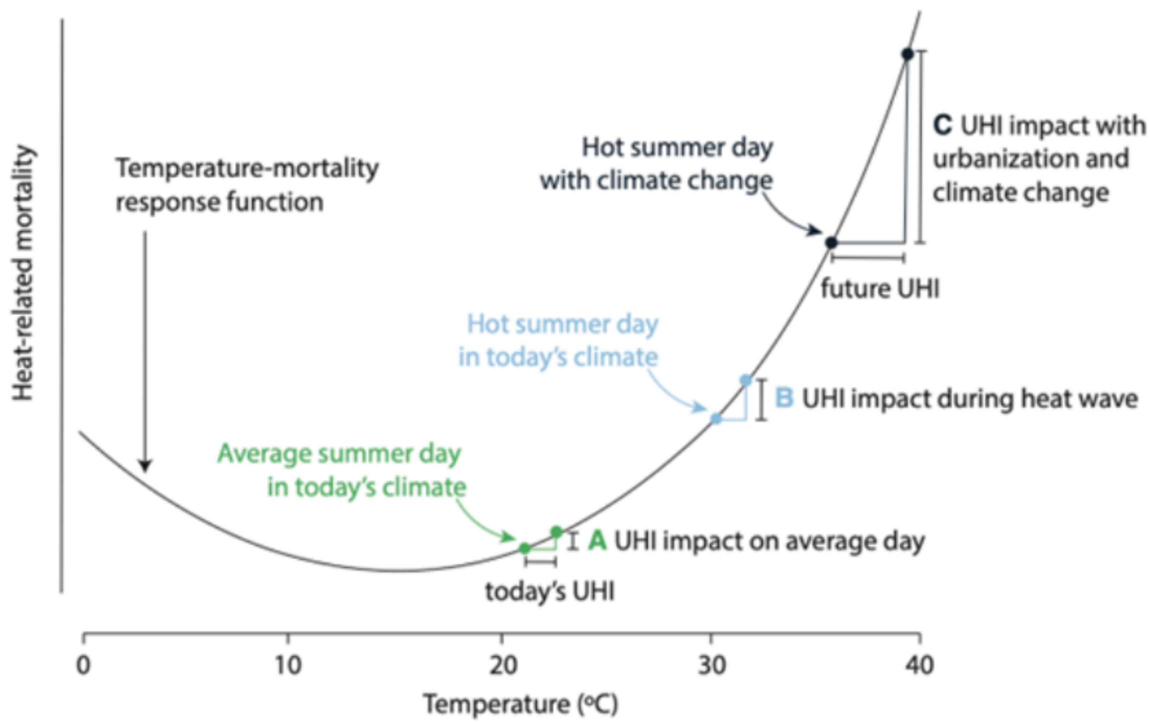

Figure 3. Correlation Between Temperature Extremes and Human Mortality

Note: The figure illustrates the U-shaped association between temperature and human mortality. It seems in the normal weather conditions on summer in today's climate, the impacts of UHI connection with health issues stay in a moderate condition (part A), while the UHI intensity increase during heat waves the condition of health risk change to the shape of (B), and if it turn to the worsen scenario like further UHI caused by cities development and climate change, higher rate of heat-related mortality (magnitude C).(Druckenmiller, 2023).

This thesis highlights only a selection of the primary adverse impacts of the Urban Heat Island (UHI) effect, acknowledging that numerous additional issues may also be associated.

1.3. Research Objectives and Investigative Questions

This research aims to analyze the spatial and temporal dynamics of the urban heat island (UHI) effect in Tehran, quantify the associated land-cover changes, and selected areas for possibly implement greenery infrastructure as a mitigation strategy for reducing environmental impacts.

This thesis will address these research questions:

In which ways did the land cover and land uses change in the city of Tehran, and if these evolutions influenced the Urban Heat Island intensity or its spatial distributions?

What are the spatial and temporal characteristics of Tehran's Urban Heat Island phenomenon?

How do variations in land surface temperature correlate with different land-use categories and degrees of vegetation cover across the city?

How do seasonal cycles modulate the magnitude of the UHI effect in Tehran?

Which areas in Tehran are most affected by urban heat dynamics, and how can satellite-based spatial analysis inform the prioritization of vegetation-based mitigation strategies?

Which distinct zones of Tehran are the best suited for applying green-based mitigation strategies to achieve the most significant reductions in urban temperatures?

1.4. Introduction of Tehran (the case study)

Iran's capital, Tehran, is located in the central north part of the country, and on the south side of the Alborz mountains, at the north side of the Dasht-e Kavir desert (Ghorbani, 2021). The coordinate of this city is between 35°30′ and 35°51′ N latitude and 51°00′ and 51°40′ E longitude(Bokaie et al., 2016). The elevation of the city varies from south to north, approximately between 1050 m and about 2030 m, respectively, leading to different microclimatic zones (Zargari et al., 2025). Northern parts of the city, which are above 1500 m, have experienced most of the time cooler temperatures, semi-arid weather, and have benefited from more water resources, which leads to the development of more gardens and green areas. (Hourcade & Habibi, 2005). The densely built central core (1,200–1,500 m) shows limited vegetation cover, while the southern sector (1,050–1,200 m) experiences hot, arid summers and cold winters.

The area of Tehran city is approximately 730 km² (Ali-Taleshi et al., 2021), and the expanded urban area includes nearly 1,700 km² (Nasehi & Imanpour namin, 2020). Tehran city has a population estimated at 8.73 million people. This increased to 15.98 million in 2016, when the wider metropolitan area is included (Talkhabi et al., 2024). Urban expansion has progressed southward and westward in recent decades, converting former agricultural lands and greenbelts into built-up areas.

The figure below illustrates the study area's topography and some information about the city, including its geographic location, elevation variations, and different zonal-level divisions within Tehran. This foundational spatial context supports subsequent analysis related to land surface temperature and urban heat island dynamics.

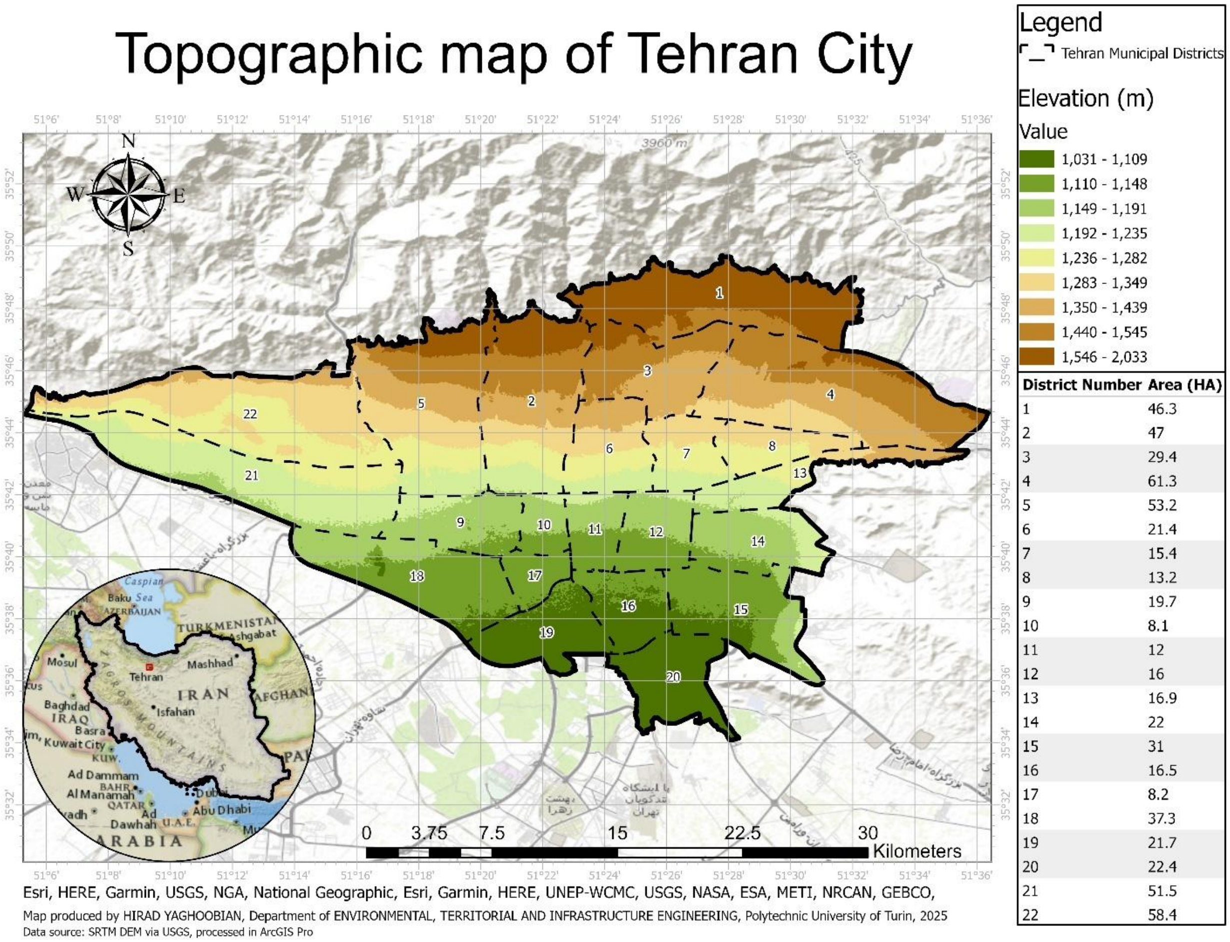

Figure 4: Elevation and Terrain Features of Tehran

The demographic growth of Tehran and its province has important implications for urban density analyses and UHI assessments. Daily inbound commuting to Tehran's central districts—driven by employment opportunities and higher income prospects—substantially augments daytime population density before workers return to peripheral towns each evening. This transient population flux increases overall energy consumption, exacerbates air pollution levels, and contributes to elevated land-surface temperatures within the metropolitan core.

Table 1. Tehran Population 1926-2016 (thousand people) (Statistical Centre of, 2016)

	1926	1936	1946	1956	1966	1976	1986	1996	2006	2011	2016
Tehran City	500	750	1000	1560	2719	4530	6042	6759	7975	8293	8737
Tehran Province	515	770	1025	1600	2806	4827	6960	8873	11228	12183	13276

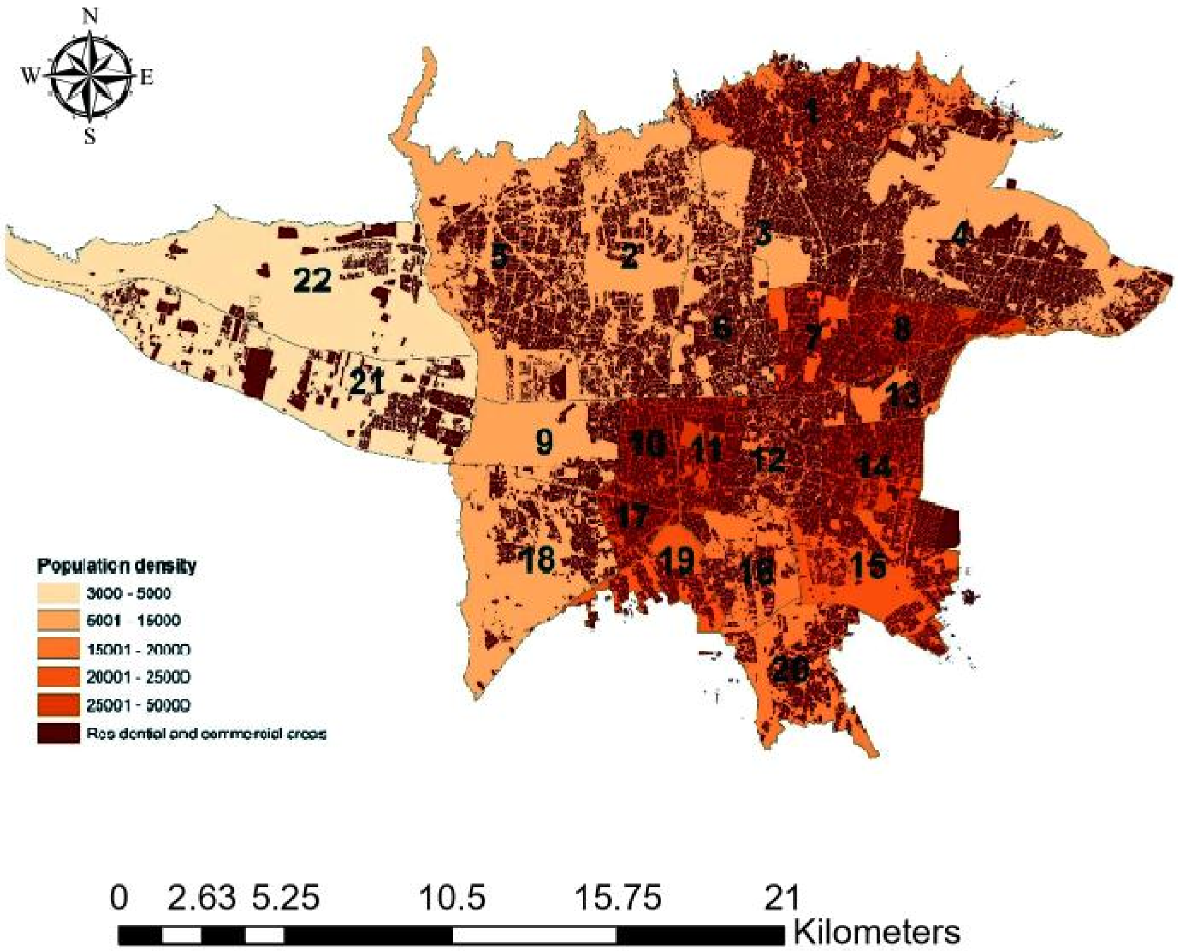

Figure 5. Population density per square kilometer of Tehran's districts in 2018 (Ghorbani, 2021)

2. Literature Review

2.1. Purpose of the Literature Review

Urban Heat Island (UHI) effects represent a growing concern in densely urbanized regions worldwide, where extensive impervious surfaces and anthropogenic heat emissions elevate urban temperatures above those of surrounding rural areas (Moghbel & Shamsipour, 2019). In arid and semi-arid cities such as Tehran, limited vegetation cover, intense solar radiation, and rapid urban expansion amplify UHI intensity, exacerbating thermal discomfort, increasing cooling energy demand, and posing significant public health and environmental challenges (Santamouris et al., 2017).UHI is thus defined as the differential between urban and rural temperatures, driven principally by land-cover alteration and reduced surface albedo (Akbari et al., 2009). As Tehran's built environment intensifies, understanding the factors that govern UHI formation and evolution becomes critical to mitigating its adverse impacts.

The aim of the literature review is to explain the total concept of measuring Urban Heat Island and the ways to mitigate the intensity in Tehran, also checking the environmental consequences of higher urban area temperature compared to rural areas. It combined the recent achievements on mitigation strategy with upgrading the ways to improve the urban vegetation covers and assessing their methods to reach a better thermal comfort, reducing the consumption of energy, especially in the city center, and reaching a better situation of urban sustainability. This part of the study brings an overview of Urban Heat Island mitigation works which are applicable in Tehran, and helping another future research to turn Tehran into a better, more resilient, and liveable place as an urban place (Razzaghmanesh et al., 2021).

This chapter includes three different key concepts: first, the causes of Urban Heat Island, second, the measurements employed to reduce its effects, and lastly, the environmental impacts, especially in the case study region. There are several causes that lead to Urban Heat Island phenomena, including: losing or limited greenery areas, low reflection (albedo) of the surfaces, and anthropogenic reasons that contribute to increasing the temperatures in urban areas. In the case study of Tehran, these reasons may be intensified due to rapid urban developments, water stress, noticeable numbers of dark surfaces, and the loss of green spaces, leading to exacerbation of the Urban Heat Island effects (Sodoudi et al., 2014).

Mitigation strategies play a vital role in solving these phenomena. The study reviews the available techniques, including planting vegetation cover based on urban greening projects, enhancement of roofs and surfaces reflection, and employing other sustainable plans to mitigate the Urban Heat Island intensity. The goals of these steps can be mentioned as reducing the heat absorbed by the city surfaces, improving cooling conditions by natural processes like evapotranspiration, and even decreasing the energy consumption. The tools will be employed and methodologies like remote sensing, Geographic Information Systems, and urban vegetation assessment that bring the important data to assess and measure these strategies and their effectiveness. (Santamouris et al., 2017).

Finally, this review will address the environmental impacts of UHI mitigation efforts, particularly the reduction of energy consumption, the improvement of urban air quality, and the enhancement of urban resilience to climate change. Effective UHI mitigation strategies can reduce the urban heat burden, improve the liveability of cities, and contribute to sustainable urban development. As Tehran faces growing environmental challenges, understanding the environmental impact of various UHI mitigation strategies will be critical for informing future urban planning and climate adaptation efforts.

By concentrating on these aspects, this literature review will establish a framework for evaluating the effectiveness of UHI mitigation strategies and guide the development of optimized approaches for Tehran's unique climate and urban structure. The review will synthesize existing research, highlight the relevance of specific tools for UHI assessment, and ultimately contribute to the broader understanding of how cities can mitigate UHI impacts in arid and semi-arid environments (Razzaghmanesh & Beecham, 2018).

2.2. Causes of Urban Heat Island (UHI) and Its Effects

2.2.1. Causes

There are several studies that show the reasons that lead to the boost of the Urban Heat Island (UHI) phenomenon:

- Decrease the amount of evapotranspiration because of the vanishing of vegetation surfaces in the city.
- Enhanced absorption of solar radiation caused by low-albedo surfaces.
- Restricted airflow resulting from increased surface roughness.
- Elevated anthropogenic heat emissions.

The major important causes of Urban Heat Island are introduced below:

There are many reasons that lead to the worsening of the Urban Heat Island (UHI) effect. One of them is low-albedo surfaces like concrete, asphalt, and roofing materials that are regularly used in urban construction, which absorb a huge amount of solar radiation and reflect it as heat, causing the surfaces and even air temperatures to rise. This heat trap can be mentioned as one of the most important factors in microclimatic warming. The other reason can be human activity known as anthropogenic heat. By the expanding the urban area and the population of the human being, the need for energy increases as well in the cities, for example, energy consumption, transportation, and industrial processes, which produce more pollutants and greenhouse gas emissions, lead to trapping longwave radiation and result in local warming, especially in megacities where there can be a very powerful correlations between the density of population and Urban Heat Island intensity. Thirdly, it is true that using air conditioners brings improved indoor comfort, but increasing the use of air conditioners can lead to worse outdoor heat temperatures. When the heat exits from cooling systems, it goes to the surrounding atmosphere, which creates a feedback loop where higher ambient temperatures lead to more energy consumption and more emissions. Fourth, urban expansion often results in widespread deforestation and vegetation loss, diminishing the natural cooling effects of shade and evapotranspiration.

In contrast, studies show that even modest increases in urban greenery can significantly lower ambient temperatures. Fifth, the urban canopy or canyon effect, caused by tall, closely spaced buildings, limits the escape of longwave radiation at night and reduces sky view factors, contributing to sustained elevated temperatures in built-up zones. Sixth, the configuration of urban areas obstructs natural wind flow, thereby reducing ventilation and heat dispersal, especially during summer and extreme heat events. Finally, air pollution from particulate matter and black carbon not only absorbs and scatters solar radiation, exacerbating surface warming, but also interferes with nighttime cooling by trapping heat and altering the urban albedo and radiation balance (Nuruzzaman, 2015).

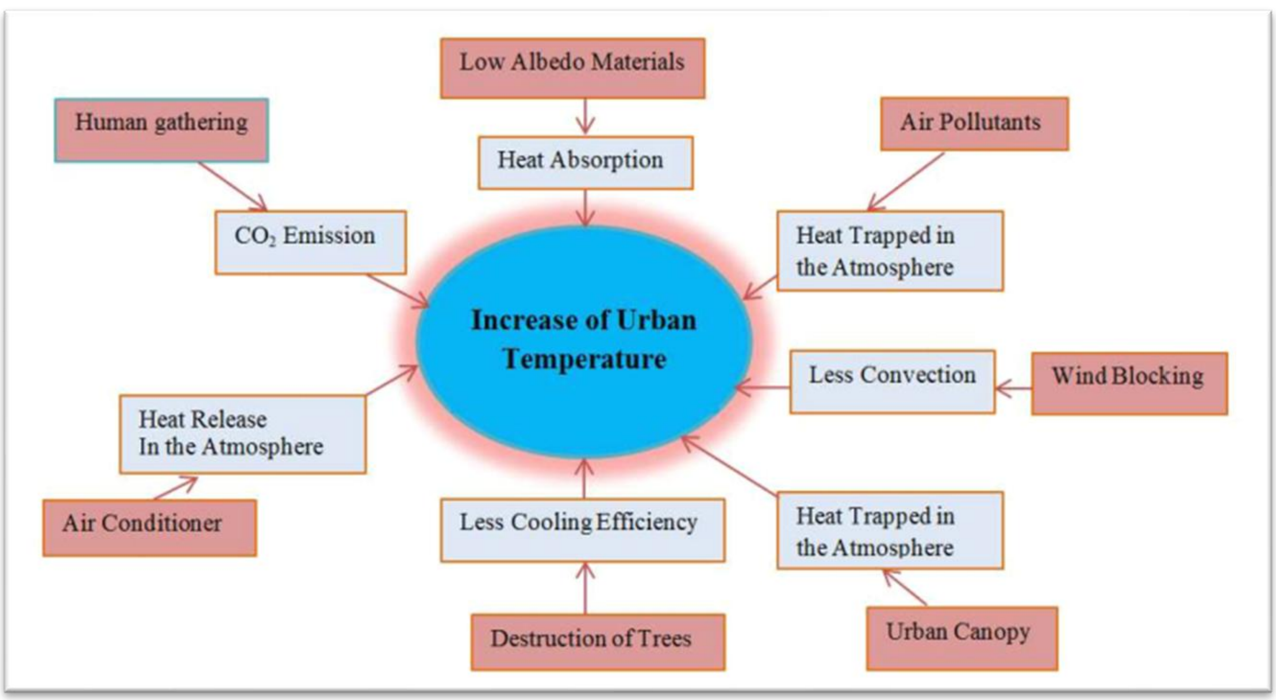

Figure 6. The Mechanism Behind Urban Heat Island (UHI) Development (Nuruzzaman, 2015)

2.2.2. Effect

The Urban Heat Island (UHI) effect has profound implications, particularly during summer, and is especially pronounced in tropical and arid regions. It causes significant discomfort for urban residents, especially those in densely populated areas. Individuals with lower heat tolerance are more prone to heat stress, which can lead to serious health issues and even fatalities (Voogt, 2004). Higher temperatures also escalate energy demands as more power is needed to cool buildings and maintain thermal comfort. (Akbari et al., 2001b) notes that energy consumption increases by 2–4% for every 1°C rise during summer. This rise burdens individuals and governments financially, while outdoor workers like construction labourers face direct exposure to intensified heat (Nuruzzaman, 2015).

The increased energy demand leads to greater fossil fuel consumption, raising greenhouse gas emissions and perpetuating a feedback loop that exacerbates UHI effects and environmental conditions. (Adinna et al., 2009) highlights that air conditioners, though essential for cooling interiors, contribute to atmospheric heat through their external heat expulsion (Nuruzzaman, 2015).

Winter benefits of the Urban Heat Island can be introduced as the rise in the urban temperature during this season helps to decrease the demand for energy consumption and heat generation. But, the advantage of winter cannot be a powerful reason compared to the negative impacts of UHI in the warmer months (Nuruzzaman, 2015).

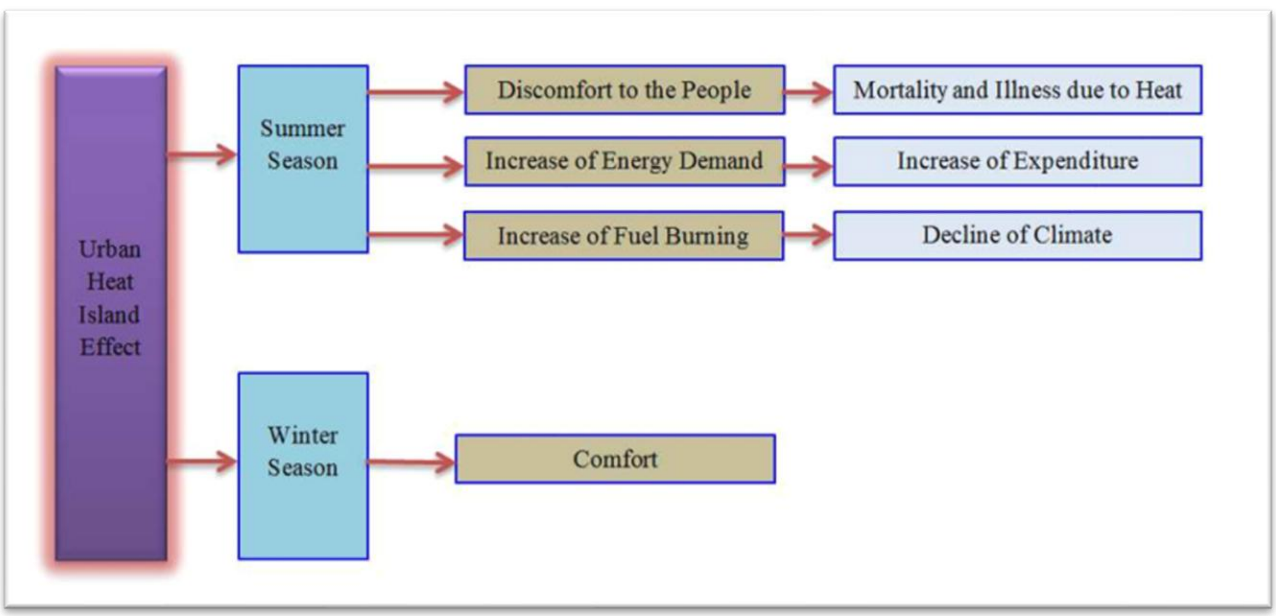

Figure 7. Impacts of Urban Heat Island Development (Nuruzzaman, 2015).

2.2.3. Urban Heat Island in Tehran

In Tehran, the weather conditions are significant in different seasons, with a hot summer from 30°C to 40°C and winter nighttime temperatures often below freezing. The lack of rainfall, with six months of dry weather in a year, and in midseason, a low-pressure system from the Mediterranean influences the area of the city. In winter, high pressure from Siberia brings cold weather to the Iranian Plateau. In summer, flow from easter, the "winds of 120 days", is linked to a thermal low-pressure system (Iran Meteorological, 2020).

Outside of summer, westerly winds prevail, although the surrounding mountains influence them. Table 2 presents the annual mean values for temperature, humidity, precipitation, and other variables recorded at Tehran-Mehrabad station (MHR) from 1980 to 2009. These data show ideal conditions for Urban Heat Island (UHI) formation, characterized by an annual mean humidity of 40% and 318 clear days annually. Tehran's geographical location contributes to significant air pollution, a key environmental issue. The Alborz Mountains, with an average width of approximately 100 km, form a barrier to the north of the city, exacerbating pollution levels (Zawar-Reza, 2008).

The climate around Tehran is semiarid, resulting in calm winds. According to Oke's classification (Oke, 1982), such weather is among the conditions suitable for UHI. These circumstances are more common in summer when the synoptic controlling factors are not as strong as in other seasons, and other atmospheric perturbations are less frequent. (Zawar-Reza, 2008) note an orderly daily cycle in the planetary boundary layer in Tehran. Wind speeds are affected by systems of turbulent atmosphere and downward momentum flux in the day. The land is cooled in the evening, and a stable boundary layer is established with low wind speeds. This nighttime boundary layer extends throughout the night, increasing temperature and pollutants, significantly increasing UHI effects and pollution of the city (Zawar-Reza, 2008).

Table 2. A summary of climate data from the Tehran-Mehrabad (MHR) station, covering the period (1980 – 2009) (Sodoudi et al., 2014).

Annual mean temperature	17.5∘C
Annual mean precipitation	230 mm
Annual mean humidity	40%
Annual most frequent wind direction	West
Mean number of clear days	318
Mean number of inversion occurrences	251

Various public examinations have investigated patterns in the most extreme and lowest temperatures and precipitation across Iran. (Alijani, 2004), (Jahadi Toroghi, 2005), and (Rasooli, 2006) have broken down information from chosen stations, while (Rahimzadeh & Asgari, 2007a) and (Rahimzadeh & Asgari, 2007b) used an exhaustive arrangement of outstanding records to explore climatic patterns over the period 1951-1997. Their discoveries demonstrated critical patterns in the least and greatest temperatures and precipitation for most Iranian locales, with an expansion in the least temperatures seen at all concentrated-on stations aside from Oroomieh, situated in the northwest.

In Iran's beachfront regions, discoveries further help warming patterns, as temperature records exhibit an expansion in warm evenings, blistering days, and the recurrence of both sweltering days and evenings, while cold spells and cool days and evenings have diminished (Zarei & Tagavi, 2010). Likewise (Tagavi & Mohammadi, 2012) have affirmed a decrease in the recurrence of cold occasions and an ascent in warm occasions over many years.

Analysing the intensity and frequency of extreme climatic events is crucial for urban planning and design, particularly in Iran's semiarid regions, where the climate is fragile and susceptible to abrupt changes that can lead to devastating consequences (Zahrani, 2013). Alongside more frequent heatwaves, rapid urbanization and the associated Urban Heat Island (UHI) effects are expected to further elevate temperatures in the coming years, underscoring the need for climate-responsive planning.

The changes of land use in Tehran, especially in recent decades, from natural surfaces to built-up urban areas, are evidence that rapid urbanization can significantly change the city's surface. These new artificial materials of land cover and surfaces have influenced the amount of solar radiation absorption and led to Urban Heat Island intensity. Additionally, population growth, driven by migration from the suburbs to the expanding urban center, has accelerated urbanization, increasing the city's size and the density of built-up areas.

Unfortunately, the local wind patterns in Tehran didn't help to mitigate the Urban Heat Island. Around 70% of the winds have speeds of less than 6 knots in Tehran, and these types of winds didn't help to guarantee enough air circulation, especially in the city center and dense building areas. Powerful winds most of the time occur in spring and early autumn, which include more than 10 knots and happen in only 30% of cases. In fact, the main sources of winds often originate from the west, south, and southeast, where industrial areas exist and are active, so these winds increase the air pollution instead of reducing the contamination. However, the north side of the city near the Alborz mountains provides some cleaner and better winds, but their impacts are quite limited.

It may be predicted that climate change in the region will lead to an intensification of these kinds of problems, such as extreme weather conditions becoming more frequent than in the past. The mean maximum temperature during heatwaves between 2001 and 2011 in Tehran is always more than 38°C and is shown in Figure 8 (Sodoudi et al., 2014).

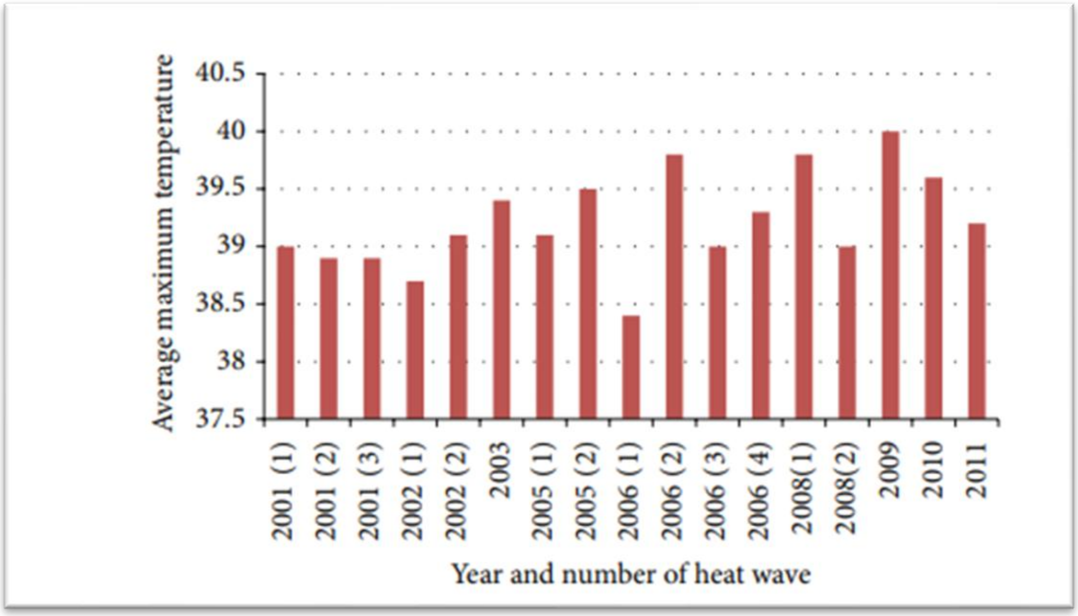

Figure 8. illustrates the average peak temperatures recorded during heat waves in Tehran between 2001 and 2011. The numbers in parentheses represent the sequence of heat waves occurring within each year. For example, Tehran experienced three distinct heat waves in 2001.

2.3. UHI Mitigation Strategies

According to Sailor, mitigating the urban heat island (UHI) effect can be approached in two primary ways: by increasing the albedo of urban surfaces or enhancing evapotranspiration. Key strategies for UHI mitigation are outlined below (D. J. Sailor, 2006c).

2.3.1. High Albedo Roofing Materials

When it comes to solar radiation reflections, dark-coloured roofs significantly absorb the radiation and heat compared to the light-coloured roofs, which reflect more of the solar radiation. The first example boosts the indoor temperature and leads to more demand for energy for cooling, whereas the lighted colours one reduces the energy consumption (Akbari et al., 2001d). So, one of the strategies can be choosing higher albedo materials for roofs to reflect solar radiation more and reduce the temperature.

However, low albedo materials for roofs absorb more heat waves, and as a result, warmer indoor spaces lead to using more air conditioners, and replacing these roofs with high-albedo materials can lead to reducing the surface temperatures without too much additional cost (Bretz & Akbari, 1998), (Rosenfeld & et al., 1992). A previous study shows that increasing the albedo from 0.20 to 0.60 can reduce the temperature of the roof by up to 25°C (Akbari et al., 1997), (Konopacki & Akbari, 1997).

Convection properties of roofing materials also play a role in the efficacy of UHI mitigation. However, a challenge associated with reflective roofs is their reduced reflectivity over time due to soot accumulation, which periodic cleaning can restore (Berdahl & Bretz, 2002).

Choosing the colour of the building surfaces is another issue. Typically, for commercial purposes, they use lighter forward, while landlords' preference is darker to cover the dirt over time (Bretz & Akbari, 1994). Another problem is related to the reflection of the light, especially for sloping designs, which can affect the driver's vision and lead to an increase in the number of car accidents. This problem is less important for flat roofs parallel to street level. So, being more careful in order to choose the colour of the roofs can be essential to minimize accidents (Bretz & Akbari, 1997).

2.3.2. High Albedo Pavements

The use of high-albedo materials for road and highway pavements can reflect more solar radiation, contributing to the mitigation of the urban heat island (UHI) effect (Akbari et al., 2001d). Selecting appropriate pavement materials with higher reflectivity can help reduce heat absorption in urban areas. Various reflective concrete surfaces with albedos ranging from 0.41 to 0.77 were tested, demonstrating their potential for UHI reduction (Levinson & Akbari, 2002a). Similarly, white cement mixtures with a higher albedo than traditional Gray cement can improve pavement reflectivity (D. J. Sailor, 2006b).

However, the effectiveness of high-albedo pavements is limited by certain factors. The sky view factor, or the portion of the sky visible from a given point, can diminish the impact, as nearby buildings may intercept reflected radiation. Additionally, vehicles often cover much of the pavement surface during the daytime, reducing its reflective efficiency (Berdahl & Bretz, 2002). As mentioned before, high-albedo surfaces may face problems like glare issues due to the reflections. It may be good for nighttime visibility and decrease the need for lights in cities, but during the day, it can have a negative impact on drivers' visibility and safety. Moreover, traffic during the years caused by vehicle movement can lead to a reduction in the pavement reflectivity and necessitate maintenance to maintain effectiveness. For gaining better results from the high-albedo surfaces, the visibility, durability, and long-term uses should be considered for better planning (Levinson & Akbari, 2002b).

2.3.3. Green Vegetation

Increasing vegetation is among the most effective strategies to mitigate the urban microclimate effects and combat the urban heat island (UHI) phenomenon (Wilmers, 1988). This can be implemented through residential tree-planting programs and municipal afforestation efforts (Dimoudi & Nikolopoulou, 2003). Vegetation mitigates the UHI effect primarily through evapotranspiration, which cools the surrounding air (Akbari et al., 2001c). Furthermore, trees play a role in temperature regulation by absorbing CO_2, helping to offset greenhouse gas emissions (Synnefa et al., 2008).

The studies of Robitu et al. and Pearlmutter et al. show that green vegetation can help reduce temperature (Robitu & et al., 2006b). (Steenveld & Heusinkveld, 2012) is another support for this study.

In city centers, where CO_2 emissions are much higher due to anthropogenic activity and population density, an increase in vegetation spaces may contribute to a reduction in temperature (Pearlmutter & et al., 2009).

Another experiment in this field by Theuwes et al. in Rotterdam, which used equipment and instruments for measuring humidity, wind speed, and temperature, confirmed that increasing 10% in vegetation surfaces can lead to a 0.6 K decrease in temperature, confirming other research which emphasizes that vegetation can have cooling effects (N. E. Theuwes & et al., 2012).

Furthermore, trees may block the air flow in city areas, which may lead to a reduction in the cooling effects of winds (Heisler, 1989). So, choosing the type and location of the vegetation should be done very carefully to have the optimal situation and maximize the benefits and minimize the negative impacts on city ventilation.

2.3.4. Shade Trees

Shade trees, characterized by their large canopies, offer substantial protection against direct sunlight, helping to cool buildings and pedestrians (D. J. Sailor, 2006d). These trees contribute to temperature reduction primarily through evapotranspiration (Akbari et al., 2001e). For example, approximately 200,000 shade trees were planted annually in the United States between 1992 and 1996 as part of efforts to mitigate the urban heat island effect, enhance air quality, and protect the climate in urban areas (Scott et al., 1999). Shade trees intercept sunlight, reducing heat absorption by buildings, lowering air conditioning demands, decreasing ambient temperatures, and improving air quality (Akbari & et al., 2001).

Despite the benefits of shade trees, they may require some costs, including planting and maintenance. But, some studies show their benefits may be reached up to 200$ over their lifetime, and their costs range between $10 and $500 per tree (Akbari et al., 2001f). However, it should consider that it takes many years for these trees to reach the level that provides enough cooling for the environment.

Other demerits of them can be mentioned as face vulnerabilities, which harsh weather events like storms may damage them and lead to damage to the building or safety risks (D. J. Sailor, 2006a). What is more, their strong roots may damage the foundations of nearby streets and buildings. Other issue of them is when we talk about UHI in megacities, the population of these urban areas is quite high, like in India and China, therefore, the limited space is a problem and careful planning can be essential based on available space, maintenance costs and their risks before planting shade trees as a cooling strategy.

2.3.5. Pervious Pavements

Impervious pavements, which do not allow water to infiltrate, limit the cooling effects of evapotranspiration (D. J. Sailor, 2006e). However, replacing these impermeable surfaces with pervious pavements that allow water infiltration can help reduce urban temperatures. When water infiltrates, it cools the pavement and has a direct impact on lowering the surrounding temperature (D. J. Sailor, 2006f), while also contributing to reduced surface runoff, enhanced groundwater recharge, and improved urban microclimates, making it a multifunctional solution for sustainable and climate-resilient city design..

2.3.6. Water Bodies

Increasing the presence of water bodies in urban areas can help lower temperatures through their evaporative cooling effects and by enhancing wind speed, as suggested by (Robitu & et al., 2006a). Water surfaces have the ability to absorb heat and reduce the Urban Heat Island intensity (Robitu & et al., 2006c). But, one study of Theuwes et al. suggested that the idea that water bodies might have a negative effect on the UHI effects means water's high thermal inertia prevents cooling at night, leading to limitations on cooling and wind speed (N. Theuwes & et al., 2012). All in all, more research in this field should be done, especially in Tehran city, to check whether the water bodies in urban areas can be an advantage or disadvantage related to the regulation of the temperature.

2.3.7. Urban Planning

One of the mitigation strategies of Urban Heat Island effects is effective urban planning. In one of the studies related to it, Yamamoto suggests an urban planning strategy for the urban areas near the rivers, which allows the airflow to the city with the help of the location of the building. It means, for example, the building with a parallel angle to the river would cause a blockage to the airflow, while the 45-degree angle in the location of the building may contribute to direct airflow to the urban areas. The most effective arrangement is when buildings are placed perpendicular to the river, ensuring airflow can reach the city from either direction. In other cities, providing ample open space and ensuring sufficient wind channels can also help reduce the effects of the urban microclimate and improve cooling (Yamamoto, 2006).

2.3.8 Green Roofs

Green roofs covering city rooftops with vegetation can significantly mitigate the urban heat island (UHI) effect. Wong highlights that roofs comprise approximately 21% to 26% of urban areas. In the city area, these types of green roofs can effectively help reduce the heat around. Actually, the green roofs absorb the heat and solar radiation and filter air, contributing to lower temperatures (Wong, 2005). The vegetation and plants in these types of roofs use the energy of heat to evapotranspiration and cool the surrounding environments.

Additionally, green roofs help delay runoff, keeping urban areas cooler longer (Getter, 2006b). Absorbing water, they maintain a cooler temperature, reducing the overall heat. Moreover, green roofs improve energy efficiency by lowering the building's energy demand and creating a more balanced energy environment (Getter, 2006a).

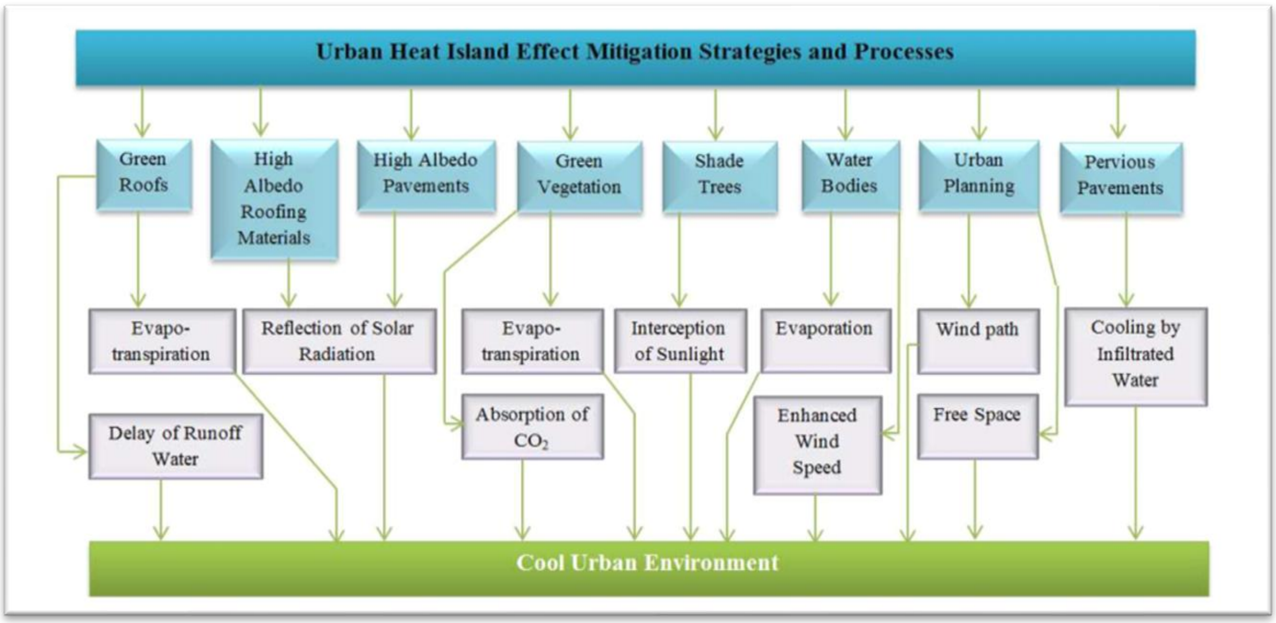

Figure 9. Strategies and Processes for Mitigating the Urban Heat Island Effect (Nuruzzaman, 2015).

2.3.9. Tehran's Current Mitigation Efforts

With the help of different mitigation strategies, the work for reducing the Urban Heat Island effects in Tehran has made progress. These actions aim to reduce surface temperature. In studies and reports that are published nowadays, a few methods are applied in Tehran to solve the Urban Heat Island intensity.

One prominent strategy involves increasing green infrastructure, such as green roofs, green walls, and urban trees. These effectively cool urban spaces by enhancing evapotranspiration, providing shade, and improving air quality. Research by Vafa and Kiani indicates that implementing green roofs in Tehran can significantly reduce urban temperatures by creating natural cooling effects and decreasing the need for air conditioning in buildings (Vafa & Kiani, 2020).

More than just green areas, installing high-albedo and permeable materials for the surface can be helpful. Reflective materials for not only roads but also pavements can lead to an increase in solar radiation reflection and a reduction of heat absorption of urban surfaces. Plus, water infiltration in the permeable surfaces allows for a decrease in temperature with the help of evaporation from the surface and turns the weather way cooler. Based on the recent findings, this strategy mitigates the

Urban Heat Island intensity and improves stormwater management more effectively in urbanized areas like Tehran (D. Sailor, 2006).

Water bodies like artificial lakes and fountains have also been incorporated into urban spaces. These bodies act as heat sinks due to water's high thermal inertia, which helps to stabilize the temperature in the surrounding areas. However, studies like those from Theuwes et al. warn that, while beneficial during the day, water bodies may inhibit nocturnal cooling when they retain heat through the night (Theuwes & et al., 2014).

What is more, the strategies in the management of the city in Tehran are going to be mitigation planning to solve the Urban Heat Island intensity. Nowadays, city planners not only try to concentrate on the angle and location of the building in Tehran for the improvement of natural airflow and wind, but also in greenery spaces to reduce as much as possible this phenomenon. These efforts are in the same direction as the sustainability aims and more liveable cities and reduce the climate change impacts.

In total, planners in Tehran try to apply a combination of these traditional and innovative methods to improve the UHI effects, like green spaces, high-albedo materials, water management systems, and other mitigation strategies. These works are part of the project of sustainability and climate resilience in Tehran planning and development. It is worth mentioning that this thesis will be exclusively concentrated on the green-based strategies among these various mitigation approaches.

2.4. Environmental Impacts of Mitigation Strategies

2.4.1. Urban Air Quality and Global Cooling

Urban areas feature various forms of greenery, including nature reserves, parks, rooftop gardens, and vertical green installations. These can be broadly classified into two main categories: natural and man-made. Over recent decades, green infrastructure has become a strategy to expand city green spaces. Examples include green roofs, green facades (Getter & et al., 2006), urban parks, and other green zones (Niachou & et al., 2001). The significance of green vegetation in influencing urban climate and mitigating urban heat was first highlighted by (Hoyano, 1988), who demonstrated its ability to reduce temperature disparities between vegetated areas and their surroundings. Since then, considerable efforts have been made to analyse the impact of green infrastructure on the built environment.

In the city, the horizontal surface, especially the unshaded ones, absorbs solar energy during summer, and around half of this absorbed energy on the surface will turn into air heat by convection, known as the ambient air temperature (Oke & Cleugh, 1987). The increases in this temperature lead to photochemical reactions between the atmospheric pollutants, which lead to smog and can affect human comfort. Furthermore, the absorption of solar energy by the surface of the building in the urban area is conducted into the building, and it may increase the cooling demand for air conditioners in these places. In the winter season, the solar radiation is lower than in the summer, which leads to absorbing less heat in the surfaces of the building (Hossieni & Akbari, 2015).

Meanwhile, changing the material of surfaces to a more reflective material (high albedo) and high thermal emittance can lead to lower surface temperature. But the cooler surfaces transfer less heat and decrease the conduction of heat into the buildings. These materials are known as cool materials, which can be used both for roofs and pavements. The impact of these cool urban surfaces on energy consumption, smog reduction, and global cooling is illustrated in Figure 10.

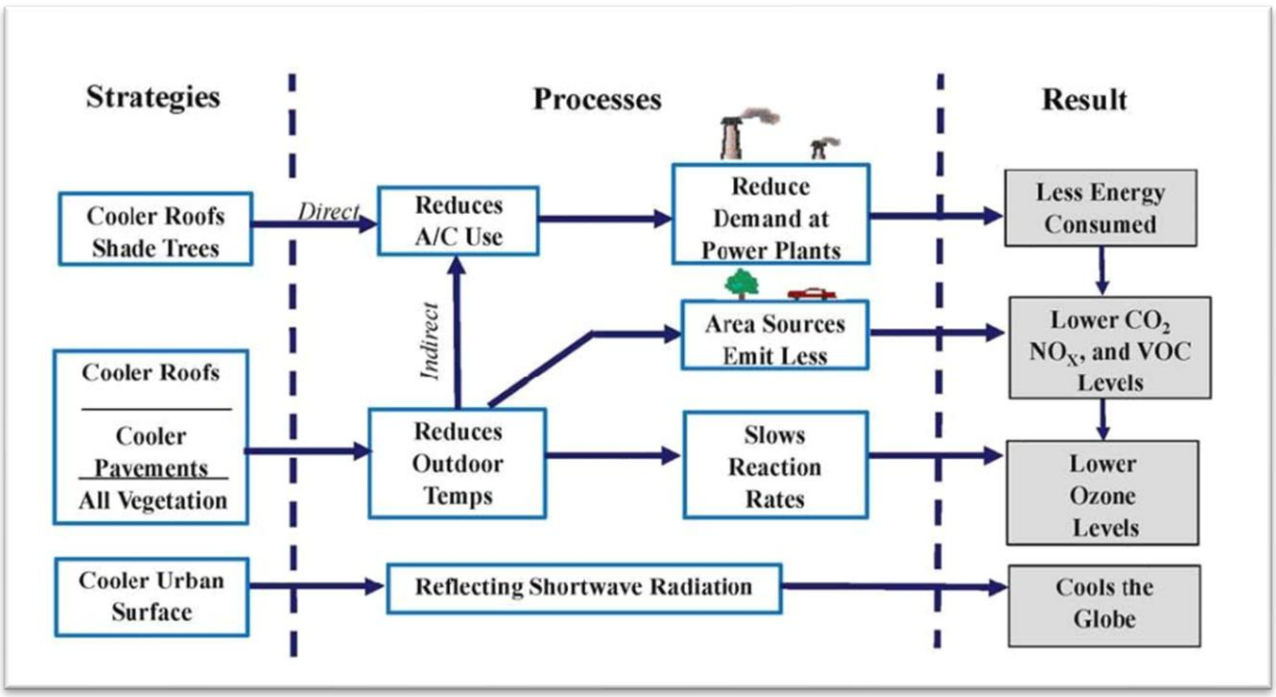

Figure 10. Environmental Impact of Urban Heat Island Mitigation Strategies (Akbari & Kolokotsa, 2016).

This figure illustrates the impact of various strategies implemented to mitigate the urban heat island effect. It includes measures such as using cool roofs and pavements, green roofs, increased vegetation, and other cooling interventions. These approaches aim to reduce surface and ambient temperatures, improve air quality, lower energy consumption, and enhance urban comfort. The figure likely compares these effects across scenarios with and without the application of countermeasures to highlight their effectiveness in urban cooling and environmental improvement (Akbari et al., 2001a).

2.4.2. The Challenges of Urban Heat Island (UHI) Mitigation

Because Tehran is in an arid area, applying a few mitigation strategies for reducing Urban Heat Island (UHI) effects brings some unique challenges, and it is not just because of its location, but also because of the resource limitation and rapid urbanization as well. These challenges can be:

As mentioned before, water limitation, especially in a populated and arid city like Tehran, is a problem. Water resources are constrained, and vegetation-based strategies for mitigation of the Urban Heat Island, like parks, gardens, and green roofs, require a huge amount of water, and it cannot be practical and logical to apply. So, reaching a balance between cooling benefits and water efficiency becomes an issue, and one should consider a sustainable irrigation system and drought-resistant plant species for these purposes (Getter & et al., 2006). As mentioned before, cool roofs, which are designed for reflecting solar radiation, can be effective in the face of Urban Heat Island mitigations.

As mentioned before, cool roofs, which are designed for reflecting solar radiation, can be effective in the face of Urban Heat Island mitigations (Santamouris & et al., 2012a). However, it can be costly both in terms of its materials and energy, and leads to challenges in Tehran:

- Material Costs: Many of these materials are not available locally and may need to be purchased. It can increase the dependency of the city or country on importing them, and it may be costly for them (Akbari & Rose, 2001b).
- Energy Costs: The manufacturing process of cool materials and their installation generates emissions and uses energy, potentially offsetting some of the environmental benefits in the short term (Taha, 1997).

2.4.3. Evaluation in Total

The intensity of the Urban Heat Island (UHI) leads to challenges for cities and people, especially in rapidly expanding urban areas like Tehran. This phenomenon can affect the environment and bring health risks when it comes to an increase in temperature, particularly in hot seasons. To fix these challenges, a few tools and frameworks have been developed for measuring the mitigation strategies. The goal of this thesis is to integrate the GIS-based spatial analysis, remote sensing, and urban greenery assessments to optimize Urban Heat Island mitigation strategies in Tehran.

One of the primary tools for evaluating UHI is remote sensing, which allows for monitoring surface temperature and urban heat distribution over large areas. Landsat satellite imagery has been extensively used for this purpose, providing high-resolution thermal infrared data that can be analysed to assess land surface temperatures (LST). Research has shown that Landsat data effectively identifies UHI hotspots and examines the temporal changes in surface temperatures, particularly in cities like Tehran, where urban sprawl significantly influences microclimates (L. Zhao & et al., 2014).

With the help of spatial and temporal analysis of Land Surface Temperature (LST), the understanding of the Urban Heat Island intensity in the different areas of Tehran is possible, which may help to find better mitigation efforts.

In addition to the remote sensing, Geographic Information Systems (GIS) tools play an important role in mapping and analysing the Urban Heat Island patterns. ArcGIS and QGIS are widely used for spatial analysis of Urban Heat Islands, because these tools help to analyse temperature data, land cover, and other interpretations that provide valuable views related to the distribution of heat all around the urban areas (Razzaghmanesh & et al., 2018b). With the help of GIS platforms, environmental factors can be analysed at the same time, and checking the correlation can guide the urban planner to make a better decision related to the strategies. These platforms can also consider some additional data, including variation of elevation, population density, and socio-economic aspects, and provide a professional overview of the Urban Heat Island's social and environmental implications.

All in all, this thesis will combine remote sensing, GIS-based spatial data analysis in different years, microclimate modelling, and land cover assessment to check the possible and better location in the city for optimizing the mitigation strategies. With the help of the data from satellites for Land Surface Temperature analysis, and other correlation analyses of parameters, we will provide a more professional overview for better understanding the situations and Urban Heat Island mitigation in Tehran. By doing so, these tools help to implement Urban Heat Island mitigation strategies and improve the urban climate and the quality of life for residents.

2.5. Case Study and Similar Examples

2.5.1. Best Globally Similar Examples to Tehran

Other cities all around the world may have a similar experience related to Urban Heat Island intensity for themselves. In this part, cities are chosen that may have several similarities with Tehran. These cities are Dubai, Cairo, and Isfahan, which provide valuable lessons. These cities have similar challenges comparable to Tehran, including hot, arid summers, rapid urban development, and limited vegetation space in urban areas. By studying their precautionary measures and strategies, we may be able to find a better solution for the case of Tehran as well.

For the case of Dubai, the combination of high-albedo materials and urban greenery has a significant effect on urban surface temperature. The advanced spatial tools in GIS help this case to achieve the target of reducing urban heat by around 2°C in critical areas of Dubai (Yao & et al., 2024a).

Cairo has focused on mapping urban hotspots using GIS to prioritize reforestation and green corridor initiatives. Research shows that increasing urban vegetation density in critical zones has reduced peak summer temperatures by up to 3°C. These efforts are especially notable for their cost-effectiveness and socio-economic alignment with the constraints of cities in the MENA region (Benaomar & Outzourhit, 2024).

Another similar example is Isfahan, in the south side of Tehran, which offers a unique experience of a combination of traditional urban design, like Persian Gardens, with modern strategies. These gardens create microclimates which reduce the local temperature by up to 5°C. Isfahan is a good examination of this model of blending, which applies the cultural heritage into the modern Urban Heat Island mitigation strategies, and achieves sustainable and cooling solutions (Yao & et al., 2024b).

2.5.2. Comparative Analysis and Local Adaptation

Like these cities in climate, Tehran faces distinct challenges such as its diverse topography and high population density. Solutions like rooftop greening, vertical gardens, and expanding public green spaces hold promises for the city. Drawing on Cairo and Dubai's use of GIS and remote sensing technologies could allow Tehran to pinpoint the most vulnerable zones for intervention. Reintroducing Persian Garden principles into Tehran's urban design could also align environmental benefits with cultural and historical preservation.

By combining these cities all around the globe, efforts with similar characteristics to Tehran urban, a better understanding and framework for applying mitigation strategies can help to address the challenges of Urban Heat Island intensity.

2.6. Research Gaps and Unresolved Issues

2.6.1. Knowledge Gaps

Despite global advances in urban heat island (UHI) mitigation research, significant gaps persist in adapting these findings to Tehran's unique urban, climatic, and socio-economic conditions. Many studies adopt generalized frameworks developed for other urban environments, often overlooking Tehran's specific challenges, such as its sprawling urban form, mixed architectural styles, and diverse microclimatic conditions influenced by its topographical complexity (Haghparast & et al., 2020).

Many studies in this field only concentrate on short-term impacts, like reducing the temperature immediately, without checking long-term impacts, especially on the environment and sustainability. In the Tehran climate, limitations of water and budget bring a serious challenge to continue with the greenery areas cooling strategies, which need high-tech materials as well. Regarding this, lifecycle impacts remain underexplored, and more studies in this field seem to be urgent (W. Zhao & et al., 2014).

Another critical gap is the disconnect between traditional Persian architectural practices, such as gardens and courtyards, and modern UHI mitigation research. These traditional methods have historically provided effective passive cooling and could offer sustainable solutions when integrated with modern urban planning. However, despite their cultural relevance and climatic adaptability, they are often overlooked in contemporary studies (Koc & Güler, 2021).

Finally, limited access to high-resolution spatial data hinders effective UHI analysis in Tehran. Most studies in this field only concentrate on low-resolution satellite images or work on limited urban climate datasets, which fail to capture the variation of heat intensity all around the city. So, mitigation efforts remain challenging without identification of the exact points of the Urban Heat Island hotspot (Tabrizian & et al., 2021).

2.6.2. Opportunities for Contribution

This study seeks to bridge these knowledge gaps by tailoring global UHI mitigation greenery strategies to Tehran's unique conditions. This research will explore culturally relevant, context-specific solutions by integrating Persian garden principles and courtyard architecture with modern techniques such as advanced GIS mapping (Santamouris & et al., 2012b).

This work will make a key contribution by emphasizing the long-term environmental impacts and resource efficiency of UHI mitigation strategies. Such assessments will provide critical insights for policymakers and urban planners to develop robust and enduring strategies (Akbari & Rose, 2001a).

This study will use advanced spatial analysis tools, like remote sensing and high-resolution GIS, to better identify the Urban Heat Island hotspot and propose suggestions for prioritizing the areas that may have higher effects related to the intensity of heat. This data-driven approach will enhance resource allocation and improve the overall efficacy of mitigation efforts (Razzaghmanesh & et al., 2018a).

3. Research Methodology

3.1. Introduction to Research Methods

In this part, the methods used to evaluate the susceptible areas to reduce the effects of UHI will be described. To do so, open-source data, including satellite, climate, and environmental data, have been used for Statistical and spatial analysis methods. Multiple satellite datasets were utilized to derive various parameters and indices to evaluate which satellite source is most effective for analyzing the study area's urban heat island (UHI) phenomenon.

3.2. Open-Source Data and Its Utilization

In this thesis, open-source data like satellite photo Landsat 8 via USGS (United States Geological Survey) Earth Explorer, MODIS (Moderate Resolution Imaging Spectroradiometer) from NASA (National Aeronautics and Space Administration), and Sentinel-2 as part of the Copernicus Program led by the European Space Agency (ESA) are utilize for evaluation and monitoring the land surface temperatures (LST), Normalized Difference Vegetation Index (NDVI), and Urban Heat Island (UHI). In addition to that, climate data like temperature is extracted from the Statistical Centre of Iran (Statistical Center of, 2022). Finally, the urban areas data, like city construction, roads, and green areas from the open street map and Tehran data center, are also used.

3.3. Data Collection Methods

Most data are collected from satellite pictures and climate data via the Internet and climate stations in Tehran. However, local observations, such as greenery areas and green roofs, can also be mentioned for assessing the situation of UHI.

3.4. Tools and Software Used

For analysis, some practical software and tools were used, including ArcGIS Pro, Python, QGIS, MATLAB, and Excel.

3.5. Data Analysis

It is vital to analyze Tehran's climate data to better understand the dynamics of Urban Heat Island intensity and check the efficiency of the mitigation strategies. The special geographical location of Tehran can be influenced by climate changes and patterns, which lead to fluctuations in temperature and environmental challenges.

In this study, for a better understanding of the climate patterns, meteorological data from 2014 to 2024 are used with a greater concentration on temperature changes and seasonal fluctuations. This can help to check the long-term variation as well.

A clear understanding of Tehran's climate is essential for evaluating the impact of urban greenery strategies, such as green roofs and gardens, on mitigating the UHI effect. By recognizing seasonal variations and climate-related challenges, informed and sustainable urban planning decisions can be made to enhance the city's environmental resilience.

3.5.1. Analysis of Land Cover Change

Before starting to analyze the satellite data for Urban Heat Island intensity, a comprehensive overview of the land cover and land use changes can be crucial for the rest of the study. For reaching this aim, two different methods of land cover classification were used. The first one uses data from Esri | Sentinel-2 Land Cover, which is available in the ArcGIS Living Atlas of the World. The changes are related to two different years, 2017 and 2023, to check the changes in land cover over this period. The second one uses MODIS Land Cover Type/Dynamics (MODIS/MCD12Q1 Version 6.1) of 2002 and 2023 and shows the changes in land cover during this period. The table below provides specific information related to the MODIS dataset.

At the end, because of the high resolution of Esri | Sentinel-2 Land Cover, these data are used for the rest of the thesis for land cover uses and changes.

Table 3. The details of the MODIS land cover

Data Set Attribute	Attribute Value
Sensor MODIS (Terra)	MODIS/MCD12Q1 Version 6.1
Date Acquired	2002 & 2023
Temporal Resolution	Yearly
Number Dimension Raster Layers	13
Projected Coordinate System	WGS 1984 UTM Zone 39N
Pixel Size	500 m

3.5.2. Comparative Evaluation of Satellite Datasets

3.5.2.1. Sentinel-2 Dataset Description

In this section, Sentinel-2 data is sourced via the Copernicus Data Space website as part of the Copernicus program to analyze temporal variations in the Normalized Difference Vegetation Index the Normalized Difference Vegetation Index (NDVI) across Tehran. The analysis utilizes monthly datasets from Sentinel-2A and Sentinel-2B, covering the period from 2016 to 2024. These data sets are processed to Level 2A, which means that atmospheric corrections have been applied, ensuring higher data accuracy. The data are acquired by the Multi Spectral Instrument (MSI), which offers high spatial resolutions specifically 10 meters (R10m) for the bands used in this study. Furthermore, the data were selected based on a cloud cover threshold of less than 10%, thereby ensuring optimal image quality. The table below summarizes key metadata associated with the Sentinel-2 products used in this analysis.

Table 4. The details of the satellite Sentinel-2 image

Data Set Attribute	Attribute Value
Landsat Product Identifier	SENTINEL-2 (A&B)
Date Acquired	2016 - 2024
Temporal Resolution	Monthly
Projected Coordinate System	WGS 1984 UTM Zone 39N
Pixel Size	10 m

To calculate the Normalized Difference Vegetation Index (NDVI) raster files, the study employs Band 4 (Red) and Band 8 (Near-Infrared) from the Sentinel-2 dataset. It is important to note that, due to the absence of a thermal band in Sentinel-2, direct derivation of Land Surface Temperature (LST) and Urban Heat Island (UHI) metrics is not feasible with these data alone. Thus, additional satellite data are required to perform these analyses.

3.5.2.2. MODIS Dataset Description

MODIS stands for Moderate Resolution Imaging Spectroradiometer, which is one of the advanced satellite sensors onboard NASA's Terra and Aqua satellites that gives the possibility for the observation of Earth's atmosphere, land, and oceans. This data is widely used for monitoring the environment, such as vegetation and land cover, land surface temperature (LST) measurement, and other climate phenomena. The table below gives some information related to the MODIS data used for this study.

Table 5. The details of the satellite MODIS image

Data Set Attribute	Attribute Value
Sensor MODIS (Terra)	MOD13Q1 & MOD21A1D
Number Dimension Raster Layers	12 & 7
Date Acquired	2010 - 2024
Day/Night Indicator	Day
MOD13Q1	Vegetation Indices 16-Day L3 Global 250m
MOD21A1D	LST L3 Global 1km SIN Grid Day

Monthly the Normalized Difference Vegetation Index (NDVI) and LST datasets for the period 2010–2024 were downloaded from Earth data Search, providing a comprehensive temporal record for the analysis of vegetation dynamics and surface temperature variations.

The Normalized Difference Vegetation Index (NDVI) of the MODIS data set, in the years between 2010 and 2024, shows the vegetation density all around Tehran. The Normalized Difference Vegetation Index (NDVI) helps to recognize the areas with higher or lower vegetation cover, which is completely important for understanding the potential mitigation strategies of Urban Heat Island based on vegetation cover.

In this section, following the acquisition of Land Surface Temperature/Emissivity Daily L3 Global 1km SIN Grid Day data from MODIS (gsfc.nasa.gov), the dataset was organized for the period spanning 2010 to 2023. After analyzing the LST data for each month within this timeframe, the Urban Heat Island (UHI) maps were generated to visualize temperature variations. The resulting ROI-based UHI maps are presented below.

The problem of the MODIS data set related to the daily data acquisition is because it is include the multidimensional layers derived from onboard sensors, without different available bands for manually calculate or even modify the cloud cover, which is lead to the significant data gapes pixels were regularly seen in the daily data of the winter seasons, where cloud coverage affected the reliability and usefully of the dataset.

For solving this data gap issue in MODIS imagery, which may be caused by cloud cover, especially during the winter seasons, using 16-day data set products is a reliable alternative way, which improves the temporal consistency. But the other problem related to using this method is that the spatial resolutions of these data sets are quite low, which leads to a limitation of the effectiveness of analysis, especially when it comes to Urban Heat Island (UHI) study, where fine-scale spatially detailed data is essential.

3.5.2.3. Landsat 8 Dataset Description

For the analysis of the Normalized Difference Vegetation Index (NDVI), Land Surface Temperature (LST) and Urban Heat Island (UHI) effect in Tehran, Landsat 8 imagery was utilized. The table below presents detailed information regarding the Landsat 8 data acquired for this study.

Table 6. The details of the satellite Landsat-8 image

Data Set Attribute	Attribute Value
Landsat Product Identifier	LC08_L2SP_164035
Date Acquired	2014 - 2024
Land Cloud Cover	11
Day/Night Indicator	Day
Satellite	8
Projected Coordinate System	WGS 1984 UTM Zone 39N
Grid Cell Size Thermal/Reflective	30
Sensor Identifier	OLI & TIRES

Landsat 8 provides high-resolution imagery (30 meters), which is useful for analyzing Land Surface Temperature (LST) and Urban Heat Island (UHI) in urban areas. However, one of the main problems in using this data over time is cloud cover. In many months, especially during winter, cloud cover affected image quality and reduced the reliability of the data. Because of this, not all monthly images could be used, and only those with acceptable quality were selected for analysis to ensure accurate results.

3.5.3. Selection of Primary Datasets for LST, UHI, and NDVI Analysis

Based on the comparative evaluation of satellite datasets presented earlier, Landsat 8 was selected as the primary data source for Land Surface Temperature (LST) and urban heat island (UHI) analysis. Its 30-meter spatial resolution and consistent thermal bands offer a suitable balance between spatial detail and data availability for urban-scale thermal assessments.

For the aim of vegetation and land cover changes analysis, Sentinel-2 data were used, based on the high spatial resolution of 10 meters and matching with the Sentinel-2 land cover dataset. This allows for checking the direct differences between the vegetation indices (such as the Normalized Difference Vegetation Index (NDVI)) and land cover classifications at the same spatial scale, which leads to more accurate spatial and temporal correlation analysis.

The table below illustrates the summary comparisons of the different satellites and sensor datasets, which introduce both pros and cons of each of them related to data availability within the Region of Interest (ROI).

Table 7. Comparative Analysis of Sentinel-2 A&B, MODIS (MOD13Q1 & MOD21A1D), and Landsat-8 (LC08_L2SP_164035) for NDVI, LST, and UHI Analysis in the Tehran Study Area

Dataset	Temporal Coverage	Advantages	Disadvantages	Data Source & Citation
Sentinel-2 A&B (2016–2024)	~8 years	- **High spatial resolution:** 10 m pixel size provides reliable details for NDVI analysis. - **Effective cloud cover modification:** Improves the usage of dataset.	- **Shorter time span:** Limited duration for long-term analysis. - **Thermal band limitations:** lack of Thermal bands dataset, making direct LST and UHI calculations challenging.	Copernicus Open Access Hub (ESA, 2024)
MODIS (MOD13Q1 & MOD21A1D, 2010–2023)	~14 years	- **Long-term data:** Extensive temporal coverage supports robust trend analysis. - **Pre-processed products:** Ready-to-use NDVI and LST facilitate analysis.	- **Low spatial resolution:** Larger pixel size decreases spatial precision. - **No cloud modification:** Lack of modification leads to data gaps in the ROI.	NASA LAADS DAAC (NASA, 2024)
Landsat-8 (LC08_L2SP_164035, 2014–2024)	~10 years	- **Convenient data duration:** Suitable for temporal trend analysis. - **Moderate spatial resolution:** 30 m for reflective bands is acceptable for land cover studies. - **Good cloud cover modification:** Enhances data quality in many instances.	- **Cloud cover issues:** Especially in winter periods, reasonable cloud cover leads to lack of data. High % of cloud cover leads to inaccuracies in LST&UHI calculations.	USGS Earth Explorer (USGS, 2024)

3.5.4. Remote Sensing Index Calculation Methods: LST, UHI, and NDVI

Remote sensing indicators are crucial in analyzing and monitoring various land surface characteristics, providing valuable insights into environmental changes, urban impacts, and climate-related phenomena. These indicators can be broadly classified into radiometric indices, biophysical parameters, and surface properties, each derived from different spectral bands of satellite imagery.

In this part, radiometric indexes, like the Normalized Difference Vegetation Index (NDVI), are calculated with the help of different spectral bands to check the vegetation cover and health. Meanwhile, biophysical parameters, such as Land Surface Temperature (LST) and emissivity, assist in quantifying the thermal variations and surface heat, which can be vital for studying Urban Heat Islands (UHI) intensity and climate dynamics. What is more, surface features, including Proportion of Vegetation (PV), help in a better understanding of energy balance and land cover properties.

With the help of a combination of these indicators, remote sensing and GIS tools give a reasonable understanding of analyzing the land surface conditions, which can support sustainable urban planning and climate adaptation strategies. The table below shows the key remote sensing indicator, their equations, and their importance in land surface analysis for this study.

Table 8. Radiometric Indices and Surface Biophysical Parameters

Name	Purpose/Classification	Primary Use Cases
TOA	Top of Atmospheric Spectral Radiance	Atmospheric corrections
BT	Top of atmosphere Brightness Temperature	Detecting thermal anomalies
NDVI	Normalized Difference Vegetation Index	Vegetation Index
PV	Proportion of Vegetation	Land cover change
LSE	Land Surface Emissivity	Accurate thermal remote sensing
LST	Land Surface Temperature	UHI analysis
UHI	Urban Heat Island	Evaluating urbanization effects

3.5.4.1. Landsat-8 Data Overview

Landsat-8 imagery was used to analyze Tehran's Land Surface Temperature (LST) and urban heat island (UHI) effect. Landsat 8, operated by NASA and the United States Geological Survey (USGS), offers high-resolution multispectral data through its two main sensors: the Operational Land Imager (OLI) and the Thermal Infrared Sensor (TIRS). These sensors can capture a wide range of wavelengths, essential for analyzing different surface characteristics such as vegetation, land cover, and thermal radiation.

The near-infrared (NIR) and shortwave infrared (SWIR) bands can be mentioned as visible bands, which can be collected based on the OLI sensor, while the thermal infrared bands can be captured by the TIRS sensor. They have different spatial resolutions, yet most of them provide 30-meter spatial resolution, except for the panchromatic band, which has a 15-meter resolution, and the thermal bands, which have a 100-meter resolution. These datasets can be applied for different remote sensing purposes, such as temperature modeling, vegetation monitoring, and land use/land cover classification (Earth Resources & Science, 2020b).

The band designations for Landsat 8, including their respective wavelengths and resolutions, are as follows:

Table 9. Landsat 8 band designations

	Bands	Wavelength (micrometers)	Resolution (meters)
Landsat 8 band designations for the Operational Land Imager (OLI) and Thermal Infrared Sensor (TIRS)	Band 1 - Coastal aerosol	0.43 - 0.45	30
	Band 2 - Blue	0.45 - 0.51	30
	Band 3 - Green	0.53 - 0.59	30
	Band 4 - Red	0.64 - 0.67	30
	Band 5 - Near Infrared (NIR)	0.85 - 0.88	30
	Band 6 - SWIR 1	1.57 - 1.65	30
	Band 7 - SWIR 2	2.11 - 2.29	30
	Band 8 - Panchromatic	0.50 - 0.68	15
	Band 9 - Cirrus	1.36 - 1.38	30
	Band 10 - Thermal Infrared (TIRS) 1	10.60 - 11.19	100
	Band 11 - Thermal Infrared (TIRS) 2	11.50 - 12.51	100

For this study, multiple Landsat 8 images were analyzed and acquired on representative dates across different years and seasons, including summer, winter, and mid-season periods. The images were sourced from the Level 2 Surface Reflectance and Surface Temperature (L2SP) product, which provides atmospherically corrected surface reflectance and surface temperature data. This product is ideal for land cover, vegetation, and thermal analysis, including corrections for atmospheric interference and sensor-related effects. The dataset is projected in the WGS 1984

UTM Zone 39N coordinate system. The spatial resolution is 30 meters for most bands, while thermal bands are provided at a native resolution of 100 meters. These data assessed seasonal environmental dynamics, including surface temperature variation and the Urban Heat Island (UHI) effect (Earth Resources & Science, 2020a).

3.5.4.2. Calculation of Top of Atmospheric (TOA) Spectral Radiance for Landsat 8 Band 10

To calculate and reach the data of Land Surface Temperature (LST) and Urban Heat Island (UHI), for the remote sensing analysis purpose, the data were downloaded from the United States Geological Survey (USGS) Earth Explorer website, including important radiometric calibration metadata. Specifically, the radiometric calibration parameters for Band 10, the thermal infrared band, were extracted from the metadata text file (MTL).

The calibration parameters obtained from the metadata are as follows:

RADIANCE_MULT_BAND_10 = 3.3420×10^{-4} (Radiometric multiplicative scaling factor for Band 10)

RADIANCE_ADD_BAND_10 = 0.10000 (Radiometric additive scaling factor for Band 10)

K_1_CONSTANT_BAND_10 = 774.8853 (Thermal constant for Band 10)

K_2_CONSTANT_BAND_10 = 1321.0789 (Thermal constant for Band 10)

$O_i = -0.29$ (Radiometric correction offset)

These parameters are essential for calculating the Top of Atmospheric (TOA) spectral radiance, which is required as an intermediate step in deriving the Land Surface Temperature (LST). The TOA spectral radiance can be calculated using the following formula:

Equation 1. Top of Atmospheric (TOA)

$$\boldsymbol{L_\lambda} = (M_L \times Band\ 10) + A_L - O_i$$

Where:

$\mathbf{L_\lambda}$ is the TOA spectral radiance.

Band 10 refers to the pixel values from the thermal infrared Band 10 of the Landsat 8 imagery.

$\mathbf{M_L}$**:** RADIANCE_MULT_BAND_10 (3.3420×10^{-4}) is the multiplicative scaling factor that converts raw digital numbers (DN) to radiance units.

$\mathbf{A_L}$**:** RADIANCE_ADD_BAND_10 (0.10000) is the additive scaling factor that adjusts the radiance.

O_i: (−0.29) is the radiometric correction offset applied to the calculated radiance.

To perform this calculation, Band 10 is loaded into ArcGIS software. Using the Raster Calculator tool in ArcGIS, the formula is applied to each pixel of the thermal band image to compute the TOA spectral radiance across the study area. This radiance value is a crucial input for subsequent LST calculations, facilitating the conversion of TOA radiance to actual surface temperatures (Survey, 2021c).

3.5.4.3. Calculation of Top of Atmosphere Brightness Temperature (BT)

Once the Top of Atmospheric (TOA) radiance has been calculated, the next step is to derive the Top of Atmosphere Brightness Temperature (BT), which is an essential parameter for the calculation of Land Surface Temperature (LST). The BT is computed by utilizing the relationship between the TOA radiance and temperature, considering the thermal constants associated with the Landsat 8 sensor.

The formula for calculating the Top of Atmosphere Brightness Temperature (BT) is:

Equation 2. Brightness Temperature (BT)

$$BT = \left(\frac{K_2}{Ln\left(\frac{K_1}{L_\lambda} + 1\right)} \right) - 273.15$$

Where:

BT represents the Top of Atmosphere Brightness Temperature in degrees Celsius.

K_2 is the thermal constant for Band 10, with a value of 1321.0789 (from the metadata).

K_1 is the thermal constant for Band 10, with a value of 774.8853 (from the metadata).

L_λ refers to the TOA radiance, which was previously calculated using the formula for TOA (in the previous step).

The natural logarithm (Ln) is used to transform the radiance into temperature units.

The final term, -273.15, is used to convert the temperature from Kelvin to Celsius.

In this process, the TOA radiance image is input into the formula, which produces the Brightness Temperature (BT) map. Using the thermal constants K_1 and K_2 allows for the proper conversion of the radiance values to brightness temperature, critical for accurate temperature modeling and the subsequent analysis of land surface temperature variations.

The resulting BT values represent the apparent temperature of the Earth's surface as observed from the satellite, corrected for atmospheric effects, and are used as a key input for further temperature analysis in the study area (Survey, 2021a).

3.5.4.4. Calculation of the Normalized Difference Vegetation Index (NDVI)

The Normalized Difference Vegetation Index (NDVI) is a widely used spectral index for assessing vegetation health, density, and coverage. NDVI is derived from the difference between the Near-Infrared (NIR) and Red spectral bands. These bands are particularly useful for vegetation analysis due to their interaction with plant chlorophyll and leaf structure. In this study, NDVI is calculated using Band 5 (Near Infrared—NIR) and Band 4 (Red) from the Landsat 8 imagery.

The NDVI formula is defined as follows:

Equation 3. Normalized Difference Vegetation Index (NDVI)

$$NDVI = \frac{(NIR - RED)}{(NIR + RED)}$$

Where:

NDVI is the Normalized Difference Vegetation Index.

NIR corresponds to Band 5 (Near Infrared), which ranges from 0.85 to 0.88 µm.

Red corresponds to Band 4, which ranges from 0.64 to 0.67 µm.

The difference between NIR and Red is divided by their sum to normalize the values between **-1 and +1**.

This calculation is applied pixel-wise across the study area to generate an NDVI raster layer. The resulting values range from **-1 to +1**, where:

Table 10. NDVI Values Classification (Survey, 2017)

NDVI Range	Land Cover Type	Description
-1 to 0	Water Bodies	Typically indicates the presence of water, such as rivers, lakes, or oceans.
0 to 0.1	Barren Areas	Represents non-vegetated surfaces like bare soil, sand, or snow.
0.1 to 0.2	Shrubs and Grasslands	Corresponds to areas with sparse vegetation, including shrubs and grasslands.
0.2 to 0.5	Sparse Vegetation	Indicates regions with moderate vegetation density, such as shrublands or senescing crops.
0.5 to 0.7	Normal Vegetation	Healthy vegetation with moderate density, often can be found in croplands or mixed forests.
0.7 to 1.0	Dense Vegetation	Represents areas with dense, typically associated with temperate and tropical rainforests.

The NDVI raster map derived from this step is essential for further environmental analysis, including urban vegetation assessment, land cover classification, and its correlation with urban heat patterns (Survey, 2021b).

3.5.4.5. Calculation of Proportion of Vegetation (PV)

After deriving the Normalized Difference Vegetation Index (NDVI), the next step in the analysis is calculating the Proportion of Vegetation (PV). This parameter is crucial in assessing vegetation distribution, directly influencing Land Surface Temperature (LST) and the Urban Heat Island (UHI) effect. PV is calculated using the following formula:

Equation 4. Proportion of Vegetation (PV)

$$PV = \left(\frac{NDVI - NDVI_{min}}{NDVI_{max} - NDVI_{min}}\right)^2$$

Where:

NDVI: represents the normalized vegetation index for each pixel.

$NDVI_{min}$: corresponds to the NDVI value for bare soil.

$NDVI_{max}$: represents the NDVI value for dense vegetation.

Vegetation plays a significant role in regulating surface temperatures in urban environments. Higher PV values indicate densely vegetated areas, contributing to temperature reduction through evapotranspiration and shading. Conversely, lower PV values correspond to built-up areas with minimal vegetation, with higher heat retention, intensifying the UHI effect. The PV index thus provides an essential metric for analyzing vegetation coverage and its impact on urban thermal dynamics (Multiple, 2019).

3.5.4.6. Calculation of Land Surface Emissivity (LSE)

After deriving the Proportion of Vegetation (PV), the next step in the analysis is calculating the Land Surface Emissivity (LSE). Emissivity is a crucial parameter in estimating Land Surface Temperature (LST), as it represents the surface's efficiency in emitting thermal radiation. Vegetation influences emissivity, as vegetated surfaces generally have higher emissivity than bare soil.

The emissivity (E) is calculated using the following formula (Moisa et al., 2022):

Equation 5. Land Surface Emissivity

$$E = 0.004 \times PV + 0.986$$

Where:

E = Land Surface Emissivity

PV = Proportion of Vegetation

0.986 = Baseline emissivity of bare soil

0.004 = Empirical coefficient representing the increase in emissivity due to vegetation cover

Land Surface Emissivity plays a vital role in thermal remote sensing and UHI analysis, as it affects the accuracy of Land Surface Temperature (LST) retrieval.

Bare surfaces (low PV values) exhibit emissivity close to 0.986, meaning they retain and emit more heat, contributing to higher surface temperatures. Vegetated areas (high PV values) have slightly higher emissivity due to their complex structure and moisture content, helping in cooling the surface.

Integrating emissivity into the analysis allows more precise thermal assessments, allowing for a better understanding of urban temperature variations and mitigation strategies against UHI effects.

3.5.4.7. Calculation of Land Surface Temperature (LST)

The Land Surface Temperature (LST) is a critical parameter in Urban Heat Island (UHI) studies, as it quantifies the temperature of the Earth's surface. In remote sensing, LST is typically derived from Brightness Temperature (BT) obtained from thermal infrared bands, such as Landsat 8 Band 10. However, since BT is affected by the emissivity of the surface, it needs to be corrected using Land Surface Emissivity (LSE) for accurate temperature estimation.

The formula for calculating LST is as follows:

Equation 6. Land Surface Temperature (LST)

$$LST = \frac{BT}{1 + \left(\frac{10.895 \times BT}{14388}\right) \times Ln(E)}$$

Where:

LST = Land Surface Temperature (°C)

BT = Brightness Temperature (K)

E = Land Surface Emissivity (unitless)

10.895 = Effective wavelength of Landsat 8 Band 10 (µm)

14388 = Constant derived from the second radiation constant (µm·K)

Land Surface Temperature (LST) is directly related to the surface characteristics, such as vegetation, soil, and built-up areas. In UHI studies, Land Surface Temperature (LST) is used to assess the thermal environment of urban and rural areas, allowing researchers to evaluate how different land cover types affect local temperatures. By calculating Land Surface Temperature (LST), we can identify urban hotspots with a significantly higher temperature, often due to impervious surfaces and low vegetation coverage.

The higher values of the Land Surface Temperature (LST) are normally found in the built-up areas, where rare vegetation spaces and high surface cover, including buildings and roads, lead to extreme heat waves. However, the lower Land Surface Temperature (LST) values generally bring greenery areas, such as parks, gardens, and forests, which are associated with evapotranspiration and increase cooling weather.

These facts and figures help for an accurate mapping procedure of the Land Surface Temperature (LST) variations in the study area, which can lead to enhancing the understanding of the Urban Heat Island intensity and finally giving a valuable overview for mitigation strategies and urban planning (Multiple, 2019).

3.5.4.8. Calculation of Urban Heat Island (UHI) Intensity

For calculating and generating the Urban Heat Island (UHI) maps, Equation 7 was employed, which considers the Land Surface Temperature (LST), as well as the mean and standard deviation of LST across Theran, the study area. The UHI index evaluates the differences between the Land Surface Temperature (LST)of urban districts and the surrounding rural or vegetation areas. With the help of this analysis, the assessment of the intensity of the Urban Heat Island effect is possible, which can be critical for urban planning, climate mitigation strategies, and understanding the thermal environment.

The formula to calculate the UHI intensity is as follows:

Equation 7. Urban Heat Island (UHI) (Myint et al., 2021)

$$UHI = \frac{LST - LST_{mean}}{LST_{std}}$$

Where:

LST: Land Surface Temperature at a specific urban location.

LST_{mean}: Mean Land Surface Temperature of rural areas.

LST_{std}: Standard deviation of LST across the study area.

Finally, the Urban Heat Island intensity gives a standard measurement of temperature variations within the urban environment:

The higher Urban Heat Island values show very different temperatures between the urban and surrounding rural zones, which shows the powerful Urban Heat Island effects in dense built-up regions.

The lower Urban Heat Island values bring the weaker Urban Heat Island effects, which suggests the urban area has somehow a similar situation in terms of temperatures to the surrounding rural environment, often because of the high vegetation surfaces or sufficient water bodies that assist in cooling the city areas.

All in all, calculating the Urban Heat Island intensity helps better analyze and understand how rapid urbanization and expanding built-up areas can influence local temperatures and assess the spatial distribution of temperature extremes in urban areas.

These assessments are vital for proposing effective mitigation strategies with the aim of reducing the Urban Heat Island intensity, including green spaces, improving urban planning, and incorporating reflective materials into urban surfaces.

4. Results and Spatial Analysis

4.1. Introduction

This chapter continues the comparative analysis conducted in Chapter 3 regarding the spatial resolution, data availability, and suitability of various satellite products, namely Landsat 8, MODIS, and Sentinel-2. It presents the results of the selected data sets deemed most appropriate for urban heat island (UHI) assessment in the study area.

Based on chapter 3 methodological parts of this study, Sentinel-2 images are selected to analyze the land cover classification and the Normalized Difference Vegetation Index (NDVI) differences, because it has a higher spatial resolution compared to the other available datasets in the selected timeframes.

Related to the analysis of the Land Surface Temperature (LST) and Urban Heat Island (UHI) intensity, the Landsat 8 dataset was used. In this part, three different dates, each of which are from different seasons (summer, winter, and mid-season), and three different years (2014, 2019, and 2024), were chosen for the purpose of analyzing and observing the seasonal and temporal changes in thermal situation of the study area.

The goal of Chapter 4 is to give a complete model of spatial and temporal analysis of Tehran land cover dynamics, vegetation trends, and land surface temperature patterns. Plus, cross-sectional analysis and correlation analysis are used to check the relationships of indices and their effects on the Urban Heat Island intensity. Additionally, the results can be used to identify the zones with the most significant thermal anomalies or land surface changes. These steps and analysis are one of the ways to inform urban planners and other experts about prioritization and suggesting areas for mitigation strategies, particularly greenery-based interventions, to reduce Urban Heat Island intensity and enhance urban climate resilience.

This chapter identifies critical hotspots to support decision-making for sustainable urban planning.

4.2. Sentinel-2 Land Cover and NDVI Analysis

4.2.1. Land Cover Classification Comparison (2017 vs. 2023)

Basically, this thesis works on land cover and its changes with the help of two remote sensing datasets: MODIS/MCD12Q1 and Sentinel-2 image datasets. Both were initially evaluated for land cover dynamics in Tehran city. The MODIS provides the long-term dataset, and the resolution is low (500 meters), which was insufficient for the level of detail required in this research.

Therefore, Sentinel-2 imagery at 10-meter resolution was selected for the primary analysis based on clear details. So, specifically, land cover data for 2017 and 2023 were extracted from the (Esri, 2023), which offers global land cover classifications derived from Sentinel-2 data.

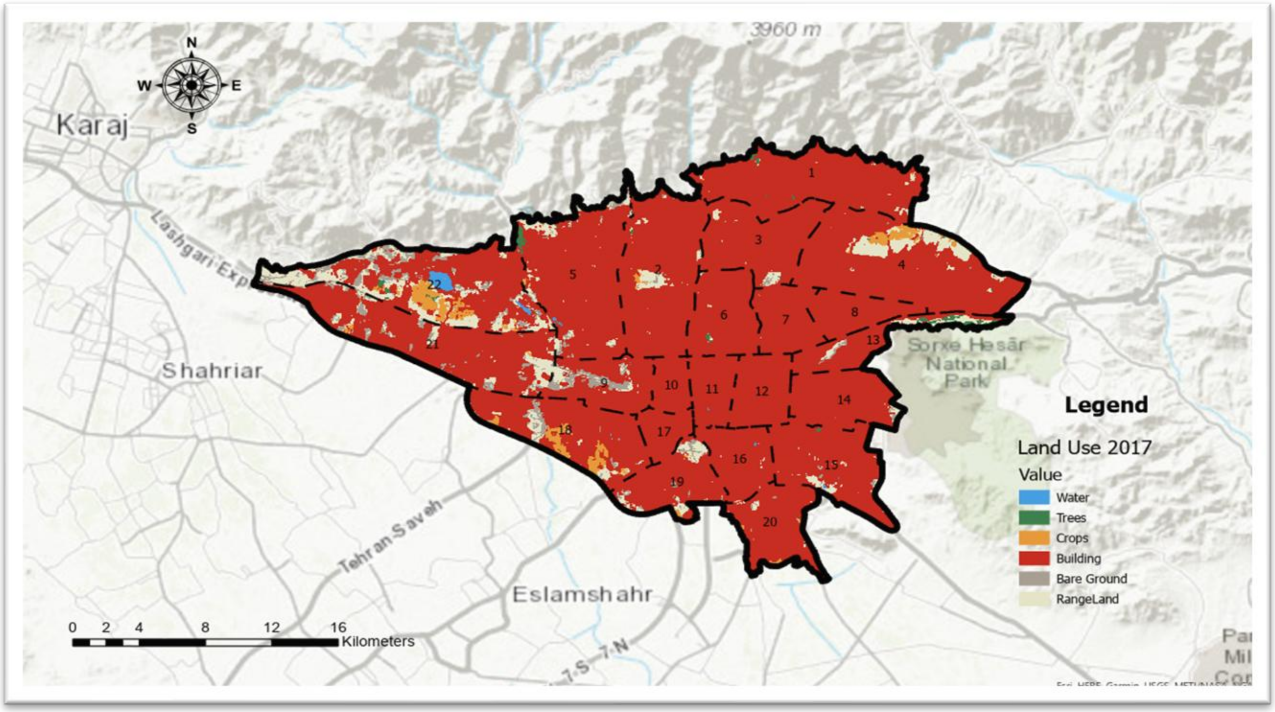

Figure 11. Tehran Land Use 2017

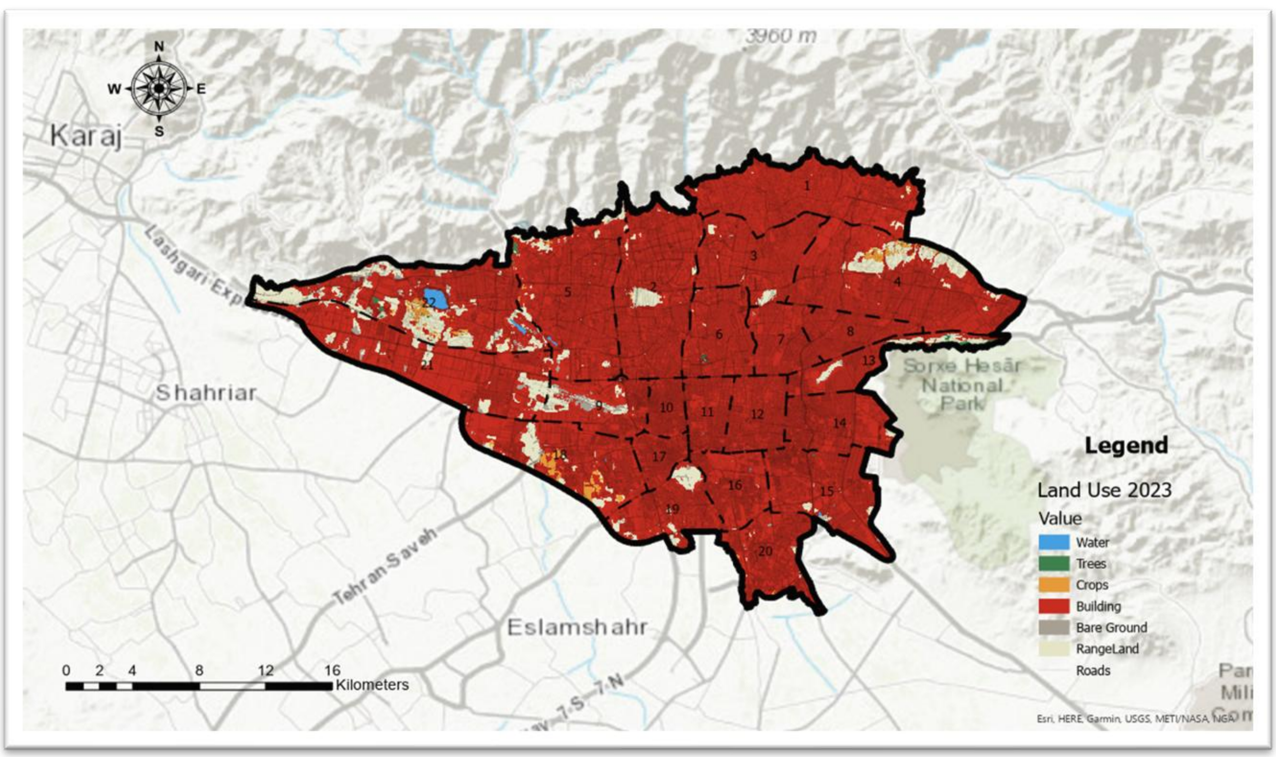

Figure 12. Tehran Land Use 2023

Table 11. Changes in Land Use in Tehran (2017-2023)

Category	Area in 2017 (km²)	Area in 2023 (km²)	Change (km²)
Water	1.50	1.20	-0.30
Trees	3.04	1.47	-1.57
Crops	11.96	6.21	-5.75
Built Area	553.01	565.33	12.32
Bare Ground	16.84	6.68	-10.15
Rangeland	42.52	47.98	5.46

The Sentinel-2 land cover data analysis for Tehran between 2017 and 2023 shows dramatic transformations associated with rapid urban development. The most significant change observed is the marked increase in built-up areas, including the expansion of the road network, driven mainly by population growth and intensified construction activities. This urban growth has predominantly occurred at the expense of natural land covers, notably vegetation types such as tree and crop cover. These have declined considerably as green spaces are converted to residential and infrastructural land uses.

Based on the data from Table 11, a reduction in the bare land coverage shows this shifting toward urbanization, which means both undeveloped and developed zones experienced expansion during this period. Accurate analysis of water surfaces remains challenging due to the seasonal and annual fluctuations in water levels.

Looking at the differences in the extent of the road network shows negligible changes during this period, which means the road network has remained generally consistent in spatial coverage, so detailed mapping is complicated by multilayered and overlapping road structures that are not easily distinguishable in satellite imagery. Although the primary focus of this study is based on Tehran's district boundaries, it is vital to mention that urbanization has happened beyond these boundaries. Rising land costs and broader economic pressures lead to the expansion of residential and commercial developments into surrounding areas, exacerbating land use changes.

What is more, an increase in industrial activities in and around the study area has likely led to an increase in CO_2 emissions and pollutants, which may affect the quality of satellite imagery analysis, so a more accurate assessment of land cover changes should be considered.

4.2.2. NDVI Pattern Comparison (2017 vs. 2023)

To assess vegetation dynamics in the Tehran metropolitan area, the Normalized Difference Vegetation Index (NDVI) datasets for April 2017 and April 2023 were retrieved from the ("Copernicus Data Space Ecosystem Browser," 2024). The NDVI was calculated using Sentinel-2 imagery and processed through ArcGIS tools, applying the standard NDVI formula equation 3.

Figure 13 illustrates the Normalized Difference Vegetation Index (NDVI) changes for these two years, which can support the future analysis of land use change and vegetation health. These raster files provide a valuable overview of the distribution and intensity of vegetation cover over the two time periods.

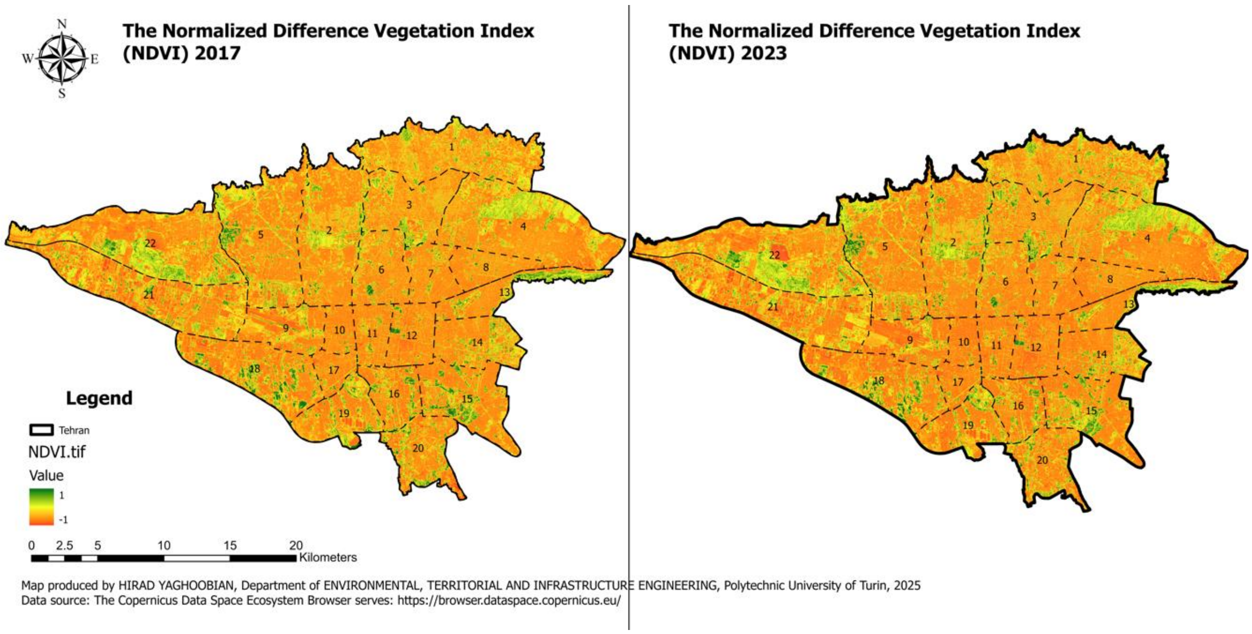

Figure 13. NDVI differences in Tehran

4.2.3. Correlation Between Land Cover Change and NDVI

Following the comparative analysis of land cover classification and NDVI datasets between 2017 and 2023, a further step was undertaken to explore the potential correlation between land cover change and vegetation dynamics. Since both NDVI and land cover change layers are raster-based, it was necessary to convert them into point data with corresponding values to perform a more accurate statistical assessment of their relationship. This enabled the use of a scatter plot to visualize and quantify the interaction between the two variables.

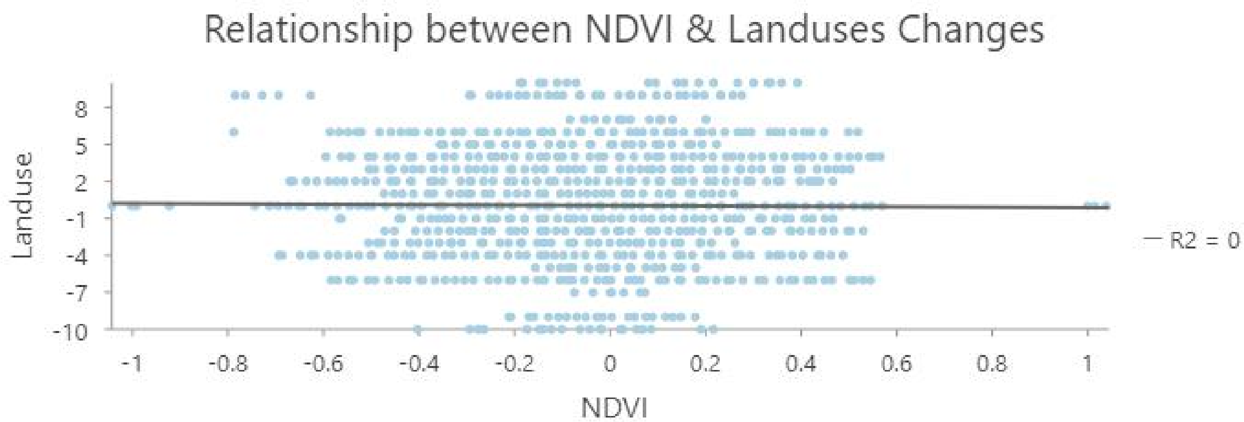

Figure 14. Statistical Association Between Vegetation Dynamics and Land Cover Change

The resulting scatter plot analysis revealed a weak negative linear relationship between NDVI change and land cover change. The regression model was defined as $y = 0.0508 - 0.1827x$, with a coefficient of determination $R^2 = 0.0002$. This very low R^2 value indicates that NDVI change accounts for only 0.02% of the variance observed in land cover change. In practical terms, this suggests that there is no meaningful statistical correlation between vegetation greenness variation and categorical land cover transitions in the analyzed sample. While the negative trend may hint at a weak association, perhaps due to vegetation loss in areas of increased urbanization, the overall relationship is negligible.

4.3. Landsat 8-Based UHI Indicators

According to the methodology detailed in Chapter 3, after processing monthly MODIS, Sentinel-2, and Landsat-8 datasets of various years, Landsat-8 imagery was selected to derive the indices presented in this section. Cloud-free Landsat 8 scenes for three representative seasons, summer, winter, and mid-season, were acquired from the USGS Earth Explorer portal ("USGS EarthExplorer," 2025) for the years 2014, 2019 and 2024. The table below summarizes the exact acquisition dates of each scene.

Table 12. Selected Landsat 8 Image Acquisition Dates for Seasonal Analysis in 2014, 2019, and 2024

Seasonality	2014	2019	2024
Mid-Season	2014.03.27	2019.05.12	2024.04.15
Summer	2014.08.02	2019.08.16	2024.08.05
Winter	2014.12.08	2019.12.22	2024.12.11

4.3.1. Seasonal NDVI, LST, and UHI Maps (2014, 2019, 2024)

As outlined in the methodology chapter, seasonal Landsat 8 imagery for the years 2014, 2019, and 2024 was processed and analyzed using ArcGIS Pro. Each dataset corresponds to a representative day within three key periods: summer, winter, and mid-season. For each scene, the Normalized Difference Vegetation Index (NDVI), Land Surface Temperature (LST), and Urban Heat Island (UHI) intensity were derived based on the procedures and formulas previously introduced.

The following figures represent the spatial distribution of these three indices in the selected seasons and years. Figures 15, 16, and 17 show the Normalized Difference Vegetation Index (NDVI) changes. Figures 18, 19, and 20 illustrate the Land Surface Temperature (LST) fluctuations. Figures 22, 23, and 24 show the Urban Heat Island (UHI) intensity during these periods in different seasons, which tell both temporal dynamics and spatial patterns of surface processes in Tehran.

The interpretation of these maps in the following sections will focus on identifying major trends, such as vegetation loss, surface temperature escalation, and the intensification or mitigation of urban heat island effects.

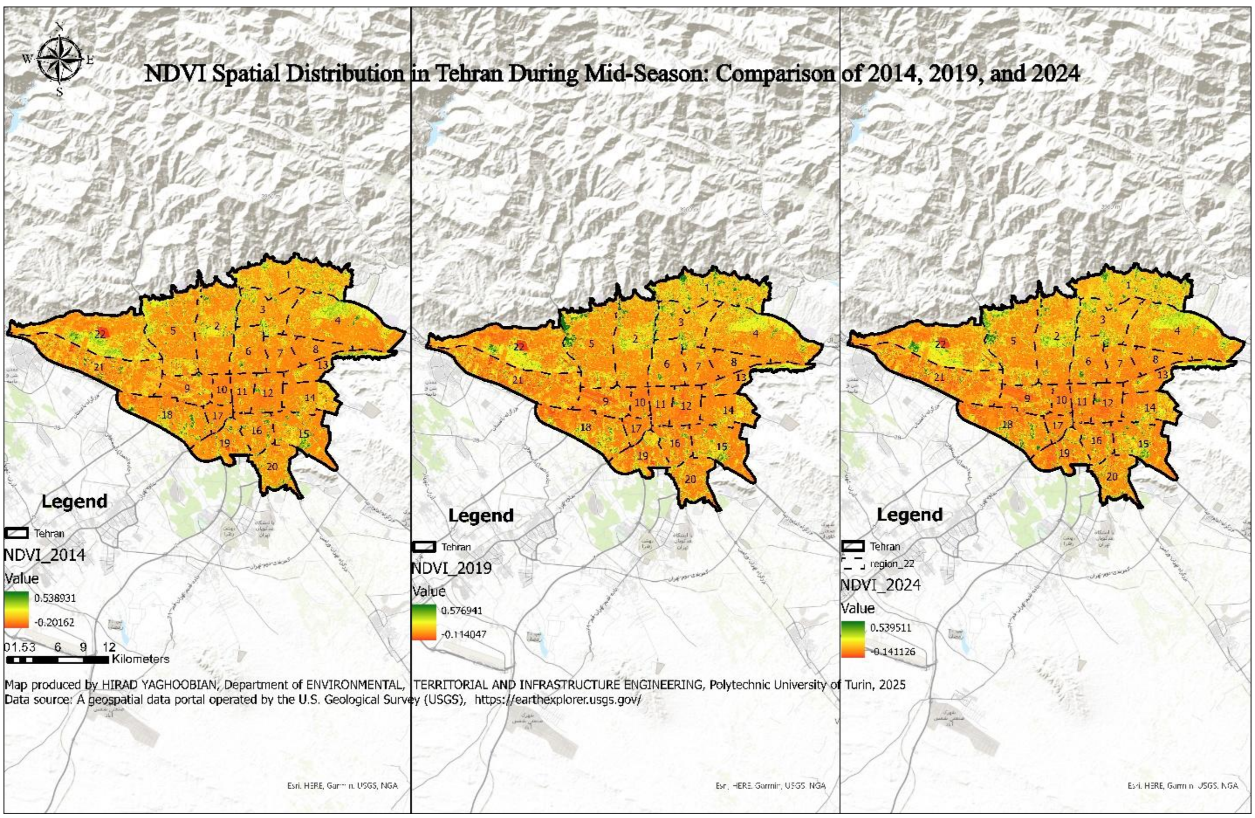

Figure 15. Comparative NDVI Maps of Tehran in Mid-Season: 2014, 2019, and 2024

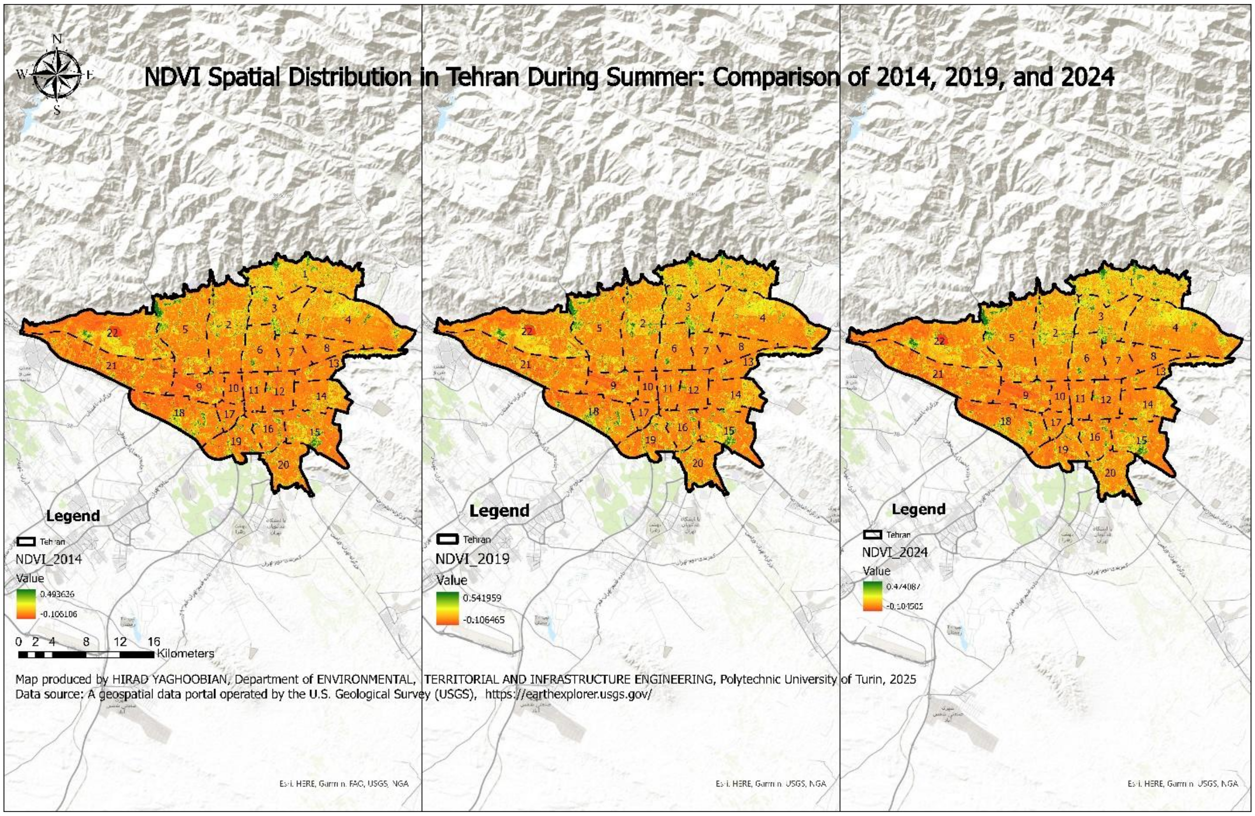

Figure 16. Comparative NDVI Maps of Tehran in Summer: 2014, 2019, and 2024

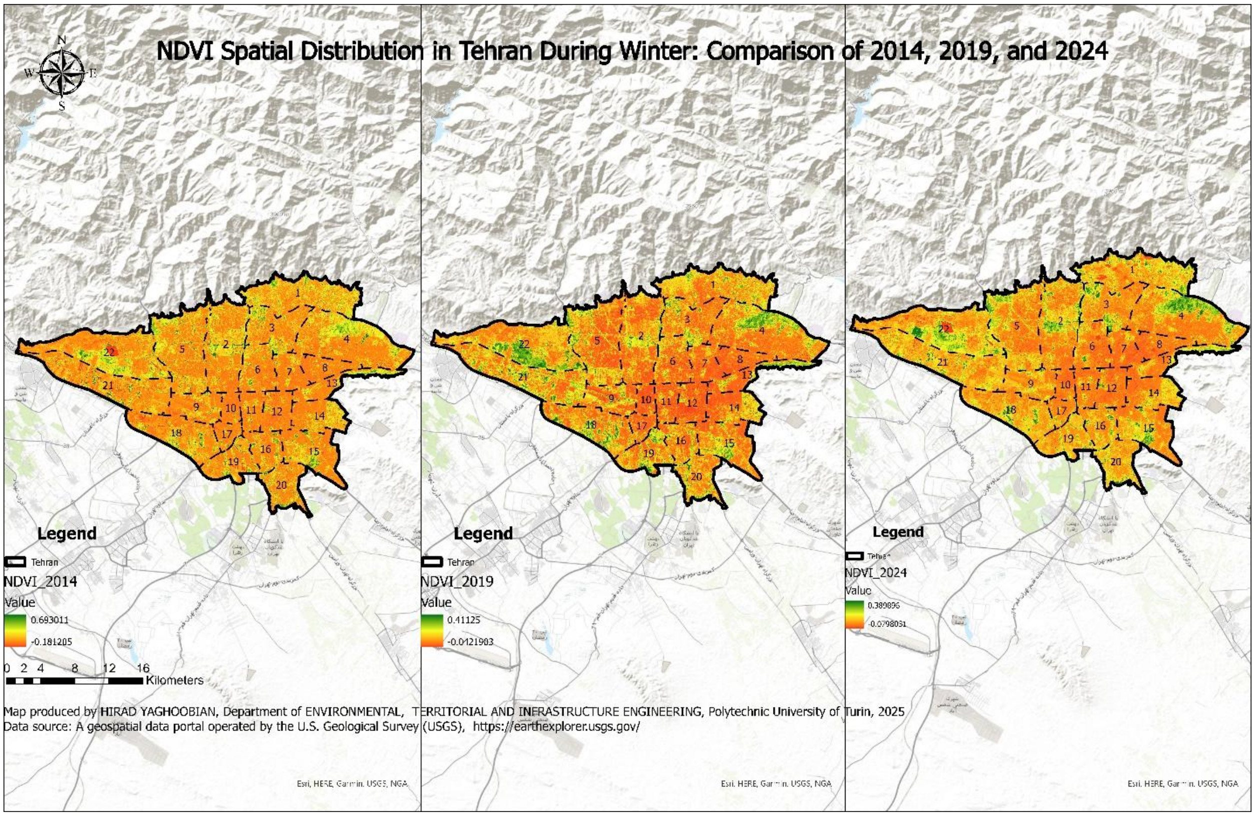

Figure 17. Comparative NDVI Maps of Tehran in Winter: 2014, 2019, and 2024

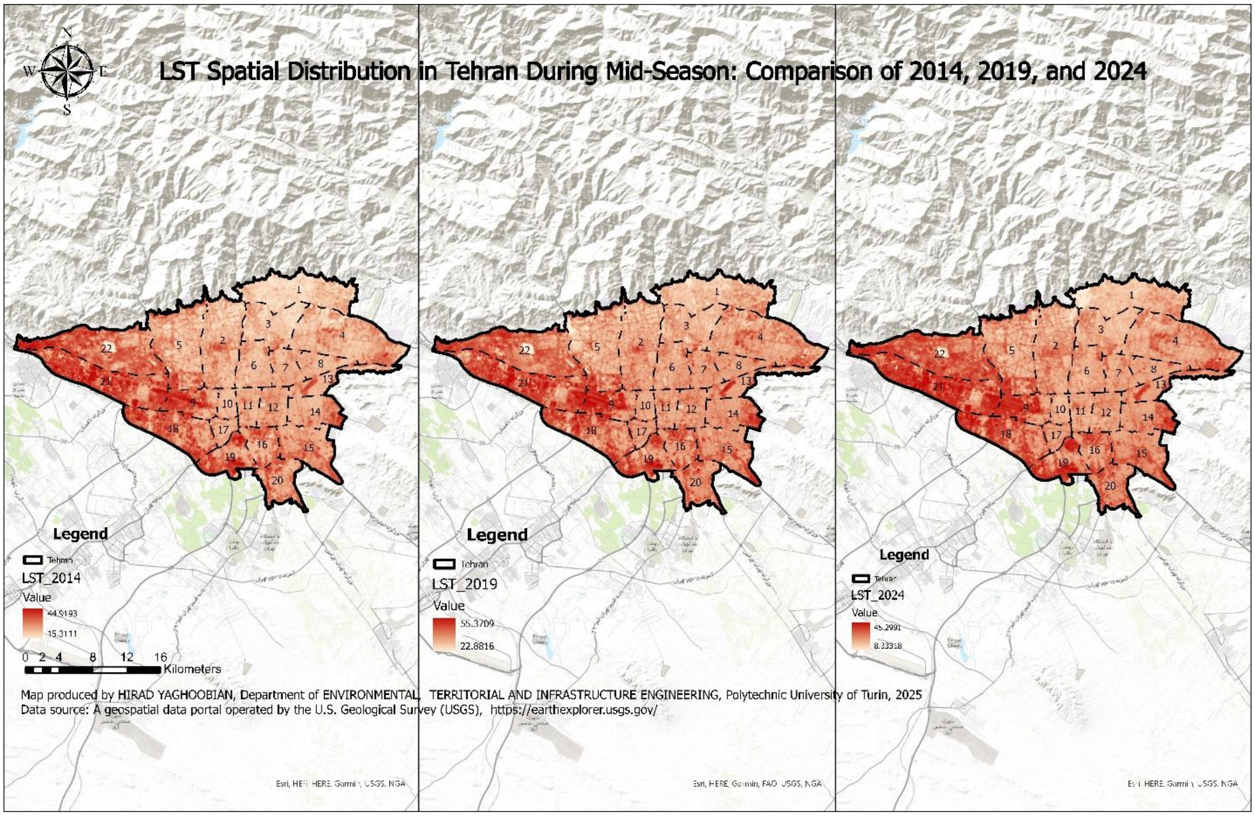

Figure 18. Comparative LST (°C) Maps of Tehran in Mid-Season: 2014, 2019, and 2024

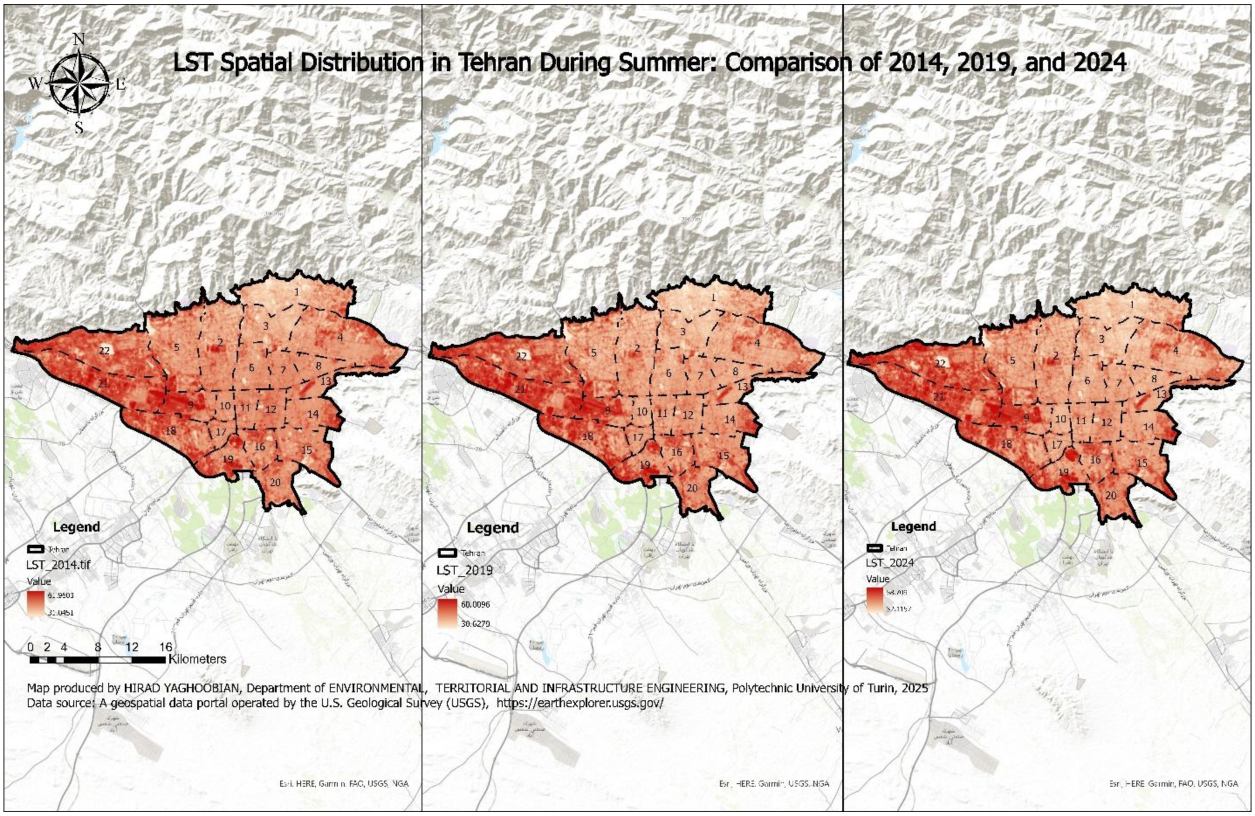

Figure 19. Comparative LST (°C) Maps of Tehran in Summer: 2014, 2019, and 2024

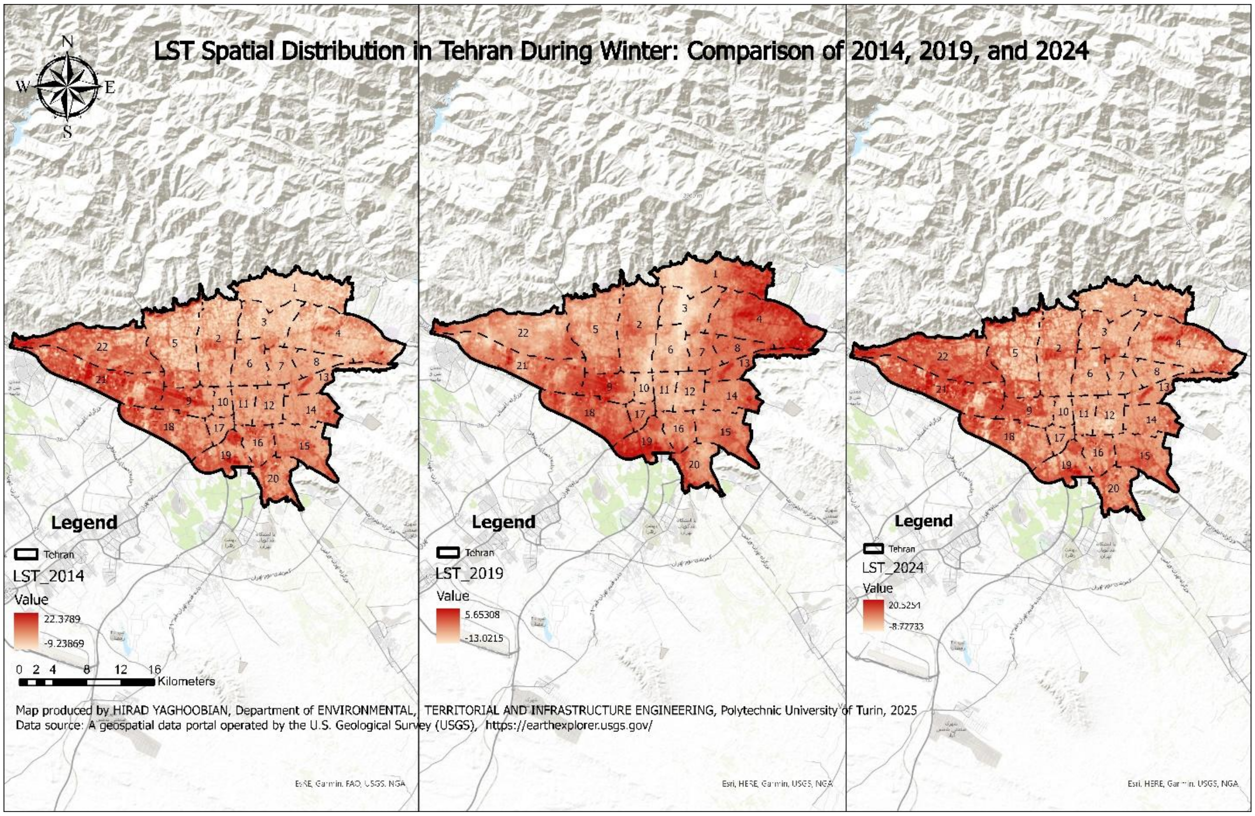

Figure 20. Comparative LST (°C) Maps of Tehran in Winter: 2014, 2019, and 2024

4.3.2. LST Change Analysis (2024 – 2014)

Following the visualization of Land Surface Temperature (LST) patterns for representative days across various seasons and years, this section focuses on the temporal comparison of LST between 2014 and 2024. By analyzing the seasonal LST differences over this period, the goal is to assess how surface temperature conditions have evolved and to identify areas that have experienced significant warming or cooling. These changes can help identify the spatial dynamics of thermal variation and highlight critical zones that are potentially affected by urban expansion, vegetation loss, or other factors. The figure below illustrates the seasonal changes in Land Surface Temperature (LST) between 2014 and 2024, covering mid-season, summer, and winter. The accompanying table presents a statistical summary of LST changes during this period for each season.

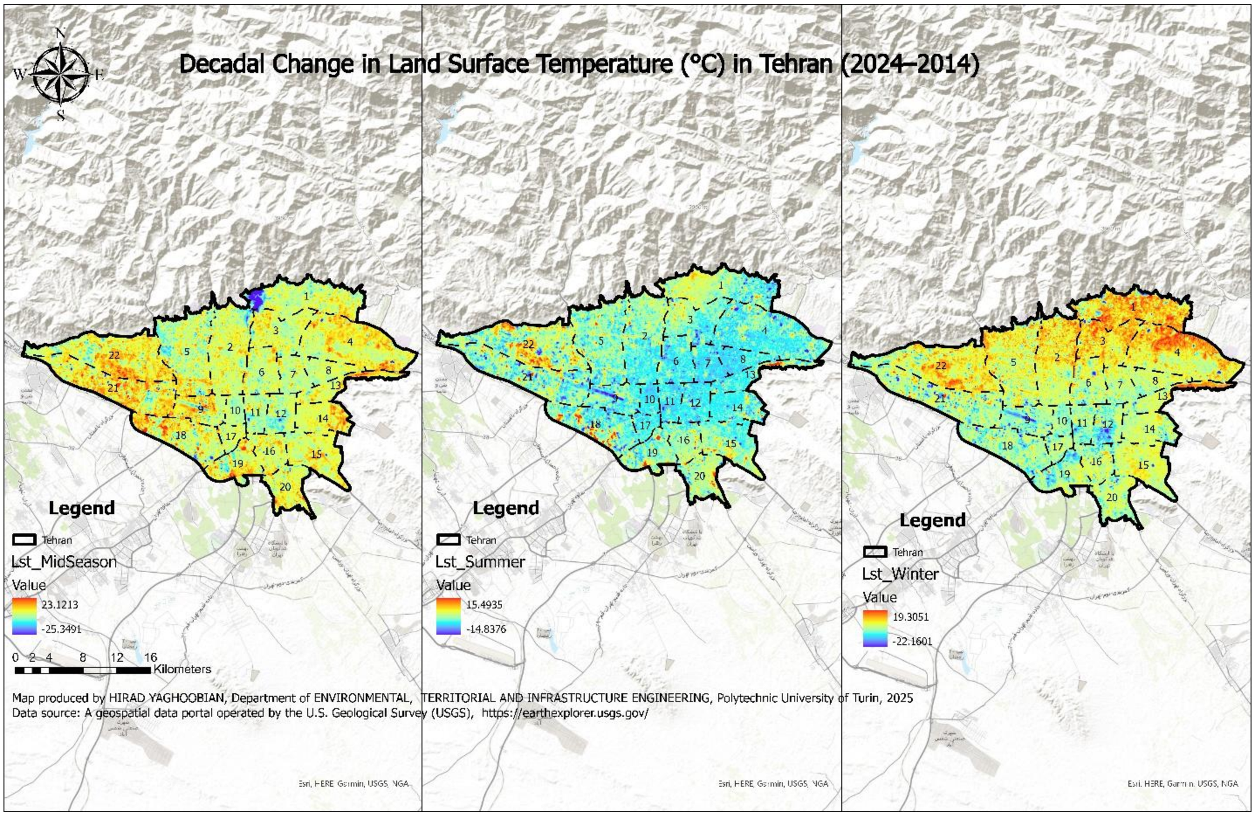

Figure 21. Decadal Land Surface Temperature (LST) Change (°C) in Tehran (2014–2024): Mid-Season, Summer, and Winter

Table 13. Statistical Summary of Seasonal LST Change (°C) in Tehran Between 2014 and 2024

Season	Min (°C)	Max (°C)	Mean (°C)	Std. Dev. (°C)
Mid-Season	-25.34	23.12	-0.24	1.68
Summer	-14.83	15.49	-1.29	1.48
Winter	-22.16	19.30	-2.32	1.26

Contrary to the typical expectation of rising temperatures due to urbanization, the results indicate a slight decrease in mean Land Surface Temperature (LST) values across all seasons, with the most notable reduction occurring during winter. This cooling trend may be attributed to several contributing factors, including seasonal climatic variability on the selected image dates, local mitigation efforts such as urban greening, and differences in atmospheric or radiometric conditions at the time of data acquisition. The number of Standard deviations remains almost constant, indicating the stability of the Land Surface Temperature (LST) across Tehran in spite of temporal changes.

4.3.3. UHI Intensity Comparison Across Years

Following the assessment of Land Surface Temperature (LST) changes over the study period, the analysis of the Urban Heat Island (UHI) intensity offers critical insight into spatial patterns of thermal stress across Tehran. UHI values were derived using the standardized anomaly method introduced in Chapter 3, where each pixel's LST was normalized against the rural mean and standard deviation. This method produces UHI intensity values typically ranging from –5 to +5, enabling a relative comparison of surface heating and cooling within the urban fabric.

The values of Urban Heat Island (UHI) can clarify some aspects. Positive Urban Heat Island (UHI) intensity values indicate that these areas are warmer than rural surrounding areas, while the negative values suggest cooler zones compared to rural areas.

According to Landsat 8 images, the datasets from 2014, 2019, and 2024 were used to calculate and visualize the Urban Heat Island (UHI) intensity.

The maps below illustrate the spatial distribution of the Urban Heat Island (UHI) intensity in Tehran for these three years and different seasons.

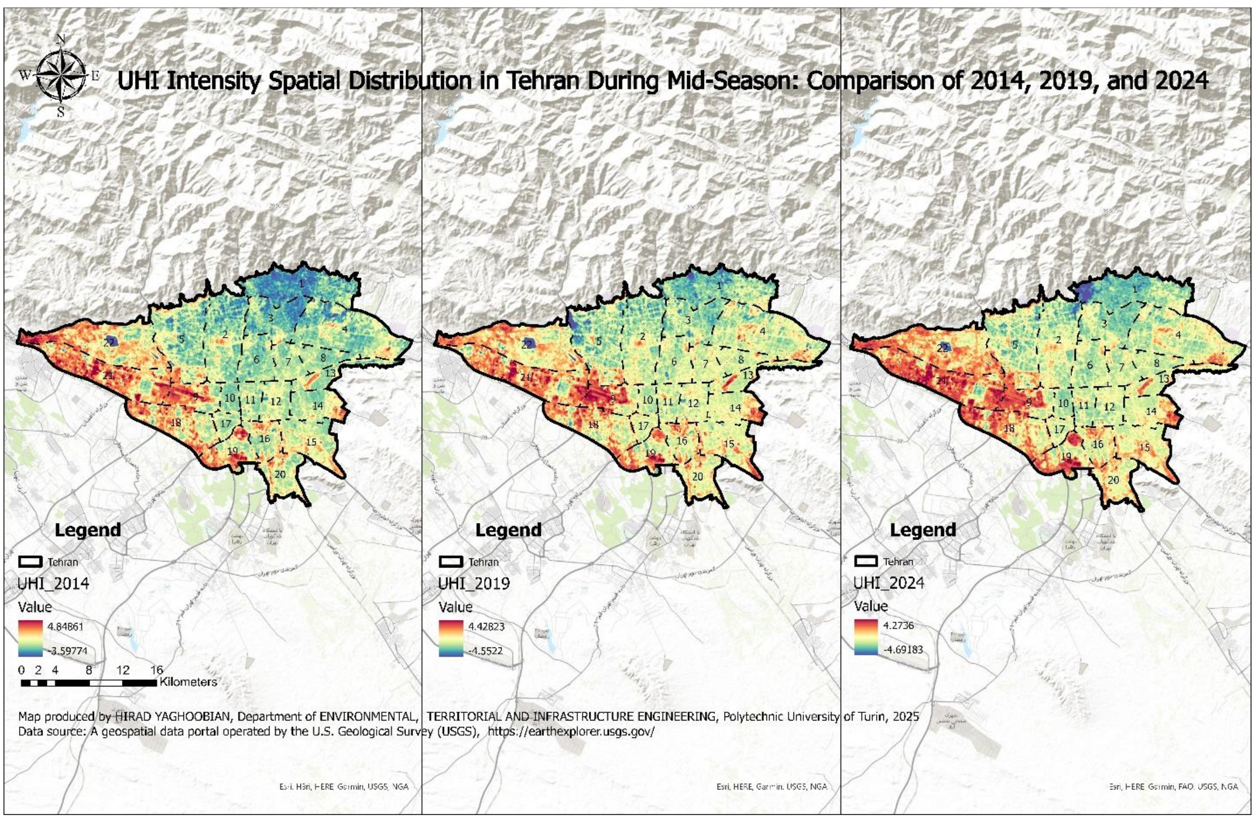

Figure 22. Spatial Distribution of UHI Intensity in Tehran for Mid-Season (2014, 2019, 2024)

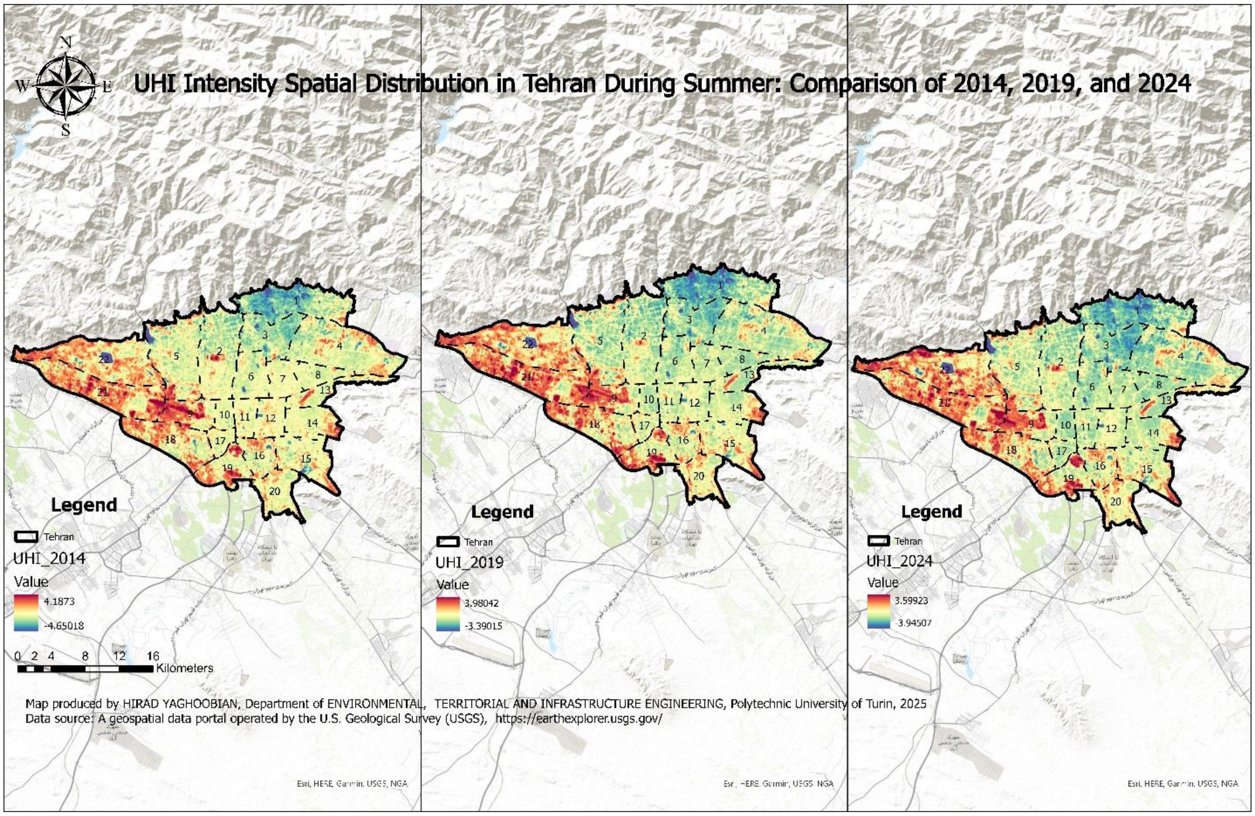

Figure 23. Spatial Distribution of UHI Intensity in Tehran for Summer (2014, 2019, 2024)

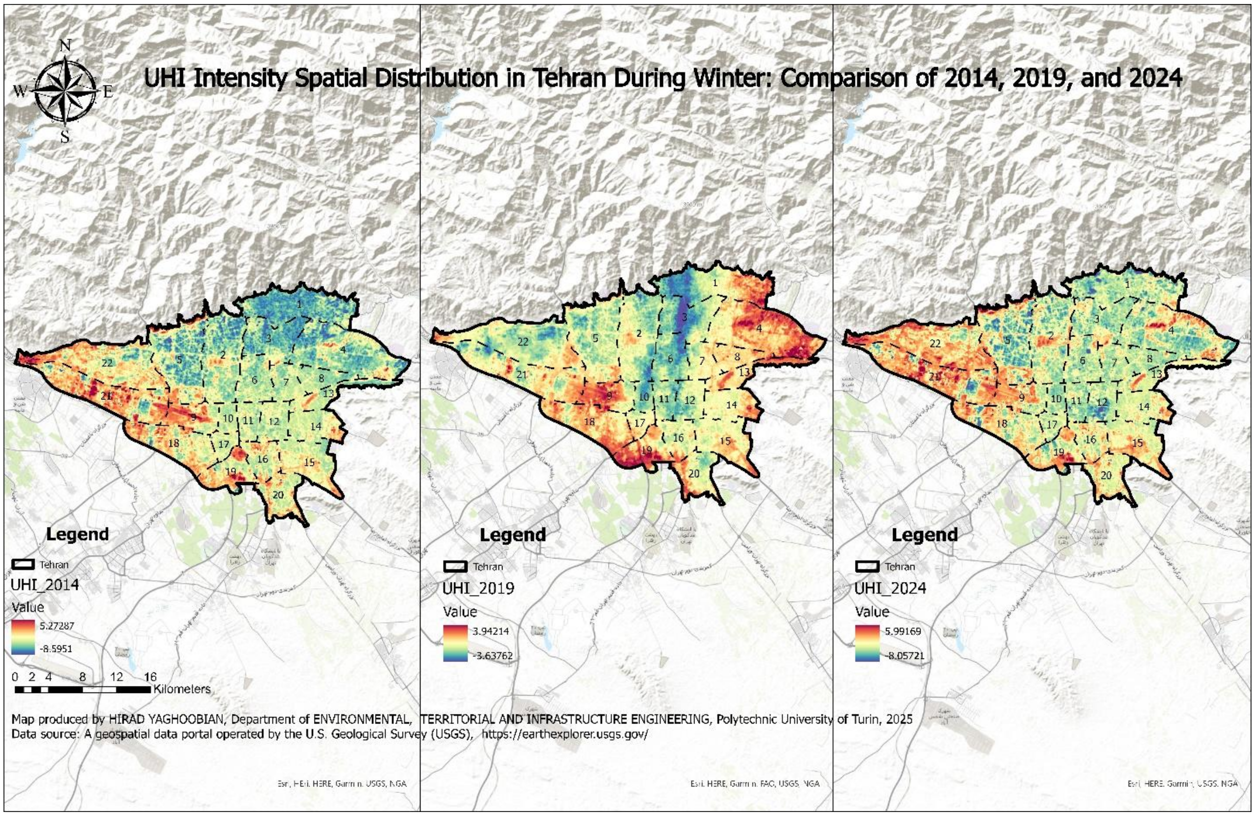

Figure 24. Spatial Distribution of UHI Intensity in Tehran for Winter (2014, 2019, 2024)

4.4. Cross-sectional Temperature Changes (2024)

To better understand the spatial distribution of surface temperatures across Tehran, a cross-sectional analysis of Land Surface Temperature (LST) was conducted for the year 2024. This analysis aims to identify areas experiencing elevated surface temperatures along both horizontal (East-West) and vertical (North-South) transects, thereby providing further insight into potential urban heat concentration zones. Such insights are crucial for prioritizing urban areas that stand to benefit the most from heat mitigation strategies.

For the East-West transect, a line was drawn between two georeferenced points:

- West Point: 508,162.45E, 3,955,733.38N
- East point: 554,800.78E, 3,955,714.39N

This transect crosses the city laterally and was applied to LST data derived from three seasonal datasets: mid-season, summer, and winter of 2024. The resulting LST profiles along this axis are presented in the figures and tables below. Peaks observed in these profiles, particularly during the summer season, may indicate localized thermal stress zones. When interpreted in conjunction with other indicators, these hotspots can help identify districts that require targeted climate adaptation interventions.

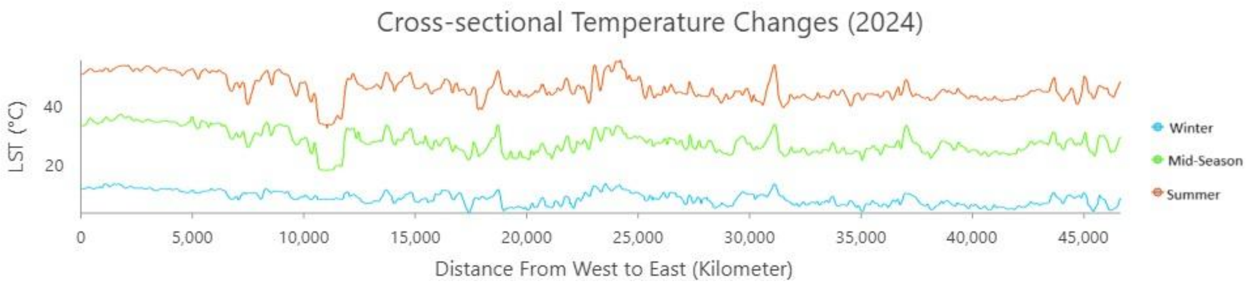

Figure 25. Land Surface Temperature (LST) Cross-sectional Profile along the East–West Transect in Tehran (Mid-Season, Summer, and Winter 2024)

Table 14. Statistical Summary of LST Values along the East–West Transect in Tehran (Mid-Season, Summer, and Winter 2024)

	LSTWinter2024 - Profile
Min	3.117
Max	13.133
Mean	8.161
Median	8.077
Sum	76129.594
Std. Dev.	2.278

	LSTMidSeason2024 - Profile
Min	17.715
Max	36.743
Mean	27.474
Median	26.927
Sum	256308.715
Std. Dev.	3.988

	LSTSummer_2024 - Profile
Min	32.15
Max	55.208
Mean	45.675
Median	44.841
Sum	426099.705
Std. Dev.	4.05

A similar method was employed for the north-south transect, extending from the northern to the southern limits of the city:

- North point: 541,801.49E, 3,964,944.71N
- South point: 538,095.02E, 3,936,505.20N

This vertical profile enables the examination of thermal variation from the higher, greener northern districts to the denser, often warmer, southern areas. The figures and summary tables below illustrate the temperature gradients along this axis, highlighting key spatial patterns that can inform future urban planning and resilience-building efforts.

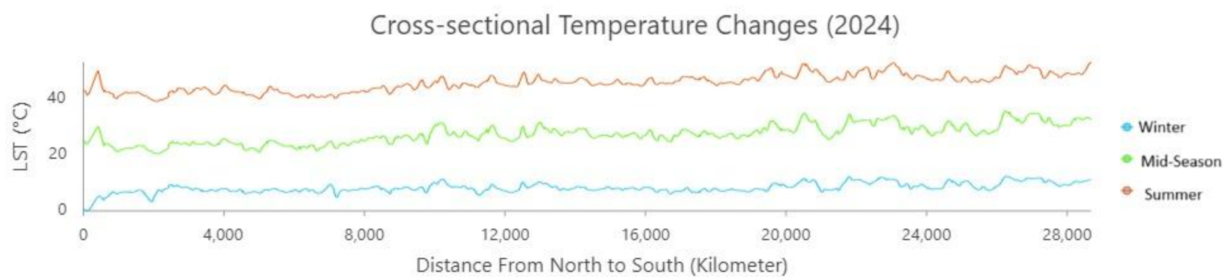

Figure 26. Land Surface Temperature (LST) Cross-sectional Profile along the North–South Transect in Tehran (Mid-Season, Summer, and Winter 2024)

Table 15. Statistical Summary of LST Values along the North–South Transect in Tehran (Mid-Season, Summer, and Winter 2024)

	Line 1 - Profile 1 Winter
Min	-1.012
Max	11.297
Mean	7.208
Median	6.901
Sum	41004.5
Std. Dev.	1.659

	Line 1 - Profile 2 Mid-Season
Min	19.332
Max	34.52
Mean	26.214
Median	25.976
Sum	149133.235
Std. Dev.	3.342

	Line 1 - Profile 3 Summer
Min	37.844
Max	51.84
Mean	44.472
Median	44.536
Sum	252998.57
Std. Dev.	3.007

4.5. Statistical Interpretation and Correlation of 2024 Data

4.5.1. Statistical Summary of LST and UHI

To support the spatial and cross-sectional analyses of land surface temperature (LST) and urban heat island (UHI) intensity conducted for 2024, this section presents a statistical overview of these variables across the three examined seasons: mid-season, summer, and winter. By summarizing key descriptive measures including, including minimum, maximum, mean, and standard deviation, the aim is to quantify the thermal characteristics of Tehran's urban environment and identify patterns of variability. These indicators offer insight into the range and distribution of surface temperatures and heat intensity across the metropolitan area, facilitating a more comprehensive understanding of seasonal thermal stress and its potential implications for urban climate adaptation.

Table 16. Descriptive Statistics of Land Surface Temperature (LST) in Tehran (2024)

Season	Min (°C)	Max (°C)	Mean (°C)	Std. Dev. (°C)
Mid-Season	8.333181381	45.29913712	27.67837804	4.123167997
Summer	32.11567688	58.70898056	46.02185709	3.524952968
Winter	-8.77732563	20.52544785	8.028163677	2.085770077

Table 17. Descriptive Statistics of Urban Heat Island (UHI) Intensity in Tehran (2024)

Season	Min (UHI)	Max (UHI)	Mean (UHI)	Std. Dev.
Mid-Season	-4.691828251	4.27359724	2.15E-07	1.000000001
Summer	-3.945068598	3.59923172	-3.21E-07	1.000000022
Winter	-8.057209969	5.991688251	-1.12E-07	0.999999974

The statistical summary of Land Surface Temperature (LST) across Tehran for 2024 reveals a clear seasonal trend. As expected, summer registers the highest surface temperatures, with a mean of approximately 46.02 °C and values peaking at over 58.7 °C, indicative of significant surface heating during the hottest months. Winter, in contrast, shows a much lower mean temperature of 8.03 °C, with a broad temperature range from –8.77 °C to 20.52 °C. Mid-season LST values fall in between, with a mean of 27.68 °C. Notably, the highest spatial variability, reflected by the standard deviation (4.12 °C), occurs during the mid-season.

The intensity of Urban Heat Island (UHI) was calculated based on the standardization, which involved each value pixel of Land Surface Temperature (LST), normalized by subtracting the mean and dividing by the standard deviation of it, in the study area. As a result, the mean Urban Heat Island (UHI) values for all three seasons are almost zero due to this formulation, while the standard deviations of them are approximately one. Furthermore, the minimum and maximum of Urban Heat Island (UHI) show areas with strong negative and positive thermal anomalies relative to the rural areas, which show the cooler and hotter urban zones, respectively.

4.5.2. NDVI–UHI Relationship and Implications

A pixel-wise correlation was performed between NDVI and standardized UHI intensity for mid-season, summer, and winter of 2024 to assess how vegetation density influences urban thermal anomalies. The following linear regression models and coefficients of determination (R^2) were obtained:

- **Mid-Season:** UHI = –2.9355 × NDVI + 0.2388 ($R^2 = 0.0218$)
- **Summer:** UHI = –5.4972 × NDVI + 0.4473 ($R^2 = 0.0766$)
- **Winter:** UHI = 10.607 × NDVI – 0.5601 ($R^2 = 0.1794$)

The R^2 value in each case indicates the proportion of UHI variance explained by NDVI: very low in mid-season and summer (≈2 % and 8 %, respectively) and modest in winter (≈18 %). A weak negative relationship during mid-season and summer implies that areas of higher vegetation tend to exhibit slightly lower heat-island intensity in warmer months. The positive winter coefficient suggests that, in colder conditions, vegetated surfaces may retain more heat than surrounding bare or built areas. Overall, the low R^2 values indicate that, while vegetation has some influence on urban temperatures, additional factors, such as surface materials, land use patterns, and built-environment geometry, also play substantial roles in shaping Tehran's thermal landscape.

4.6. Priority Suggestion Zones

With the help of all analysis which presented in this chapter, like land cover changes, assessments of Normalized Difference Vegetation Index (NDVI), levels, distributions of Land Surface Temperature (LST) , decadal changes of Land Surface Temperature (LST), and Urban Heat Island (UHI) intensity, a numbers of districts in Tehran have been identified as high-priority zones for greenery-based mitigation strategies. These districts are susceptible to more urban heat stress and are suitable for applying green infrastructure.

If all 22 districts of Tehran city are considered, districts 4, 9, 18, 19, 21, and 22 are more suitable for applying some precautionary measures. These six districts experienced low Normalized Difference Vegetation Index (NDVI), values during different seasons, high summer Land Surface Temperature (LST) values, significantly increases in Land Surface Temperature (LST) from 2014 to 2024, or have the extreme Urban Heat Island (UHI) intensity in the most recent year, and due to the fact that, the showed up more often in the analysis, it may be clear that these are the districts which more important for the future city planning and mitigation strategies.

It is important to note, however, that while six districts were identified as significant, five locations have been selected and marked on the figure below to represent suggested introductory sites for implementing green mitigation strategies. These selections are not definitive, nor do they imply exclusivity. More optimal intervention sites may exist and could be identified through the inclusion of additional variables or alternative assessment methods. Factors such as local wind direction, solar radiation reflection, surface albedo, humidity levels, and precipitation patterns, none of which were thoroughly explored in this study due to data limitations, can significantly influence heat distribution and the effectiveness of heat mitigation.

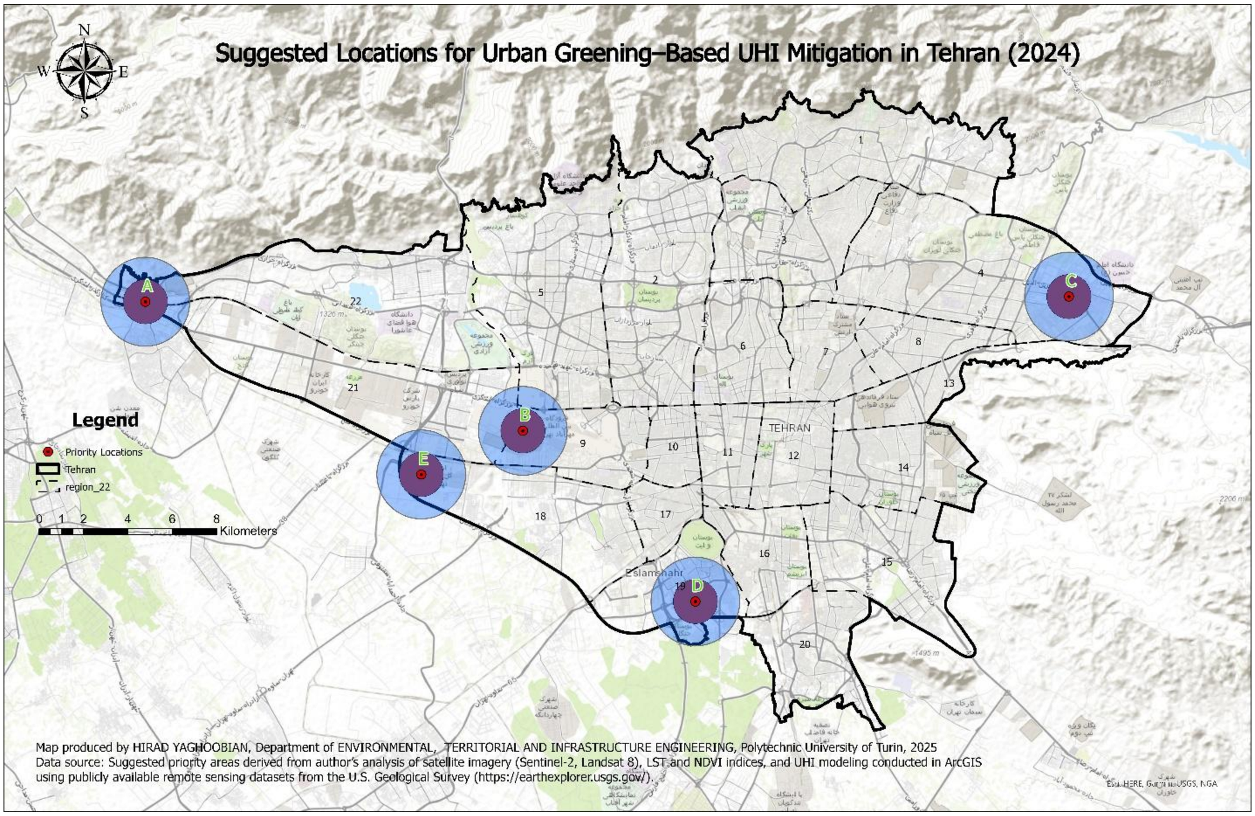

Figure 27. Suggested Locations for Urban Greening UHI Mitigation in Tehran (2024)

Table 18. Summary of Suggested Priority Locations for Urban Greening Interventions in Tehran

Point ID	Latitude	Longitude	NDVI (Summer 2024)	LST (°C, Summer 2024)	UHI Intensity (2024)	Usability
A	51.10459547	35.7431136	0.02675	50.462406	High	Industrial and Transit Zone
B	51.29266112	35.69036158	0.031984	52.60437	Very High	Aviation and Light Industrial Area
C	51.56516424	35.74394102	0.04184	45.268536	Moderate	Residential and Institutional Corridor
D	51.37830921	35.62076551	0.052335	54.246708	Very High	Commercial-Residential Urban Core
E	51.24196029	35.67272618	0.045807	48.891773	Moderate–High	Mixed-Use Urban Zone

Therefore, the zones identified in this study should be considered as informed starting points for mitigation rather than final recommendations. Future assessments integrating a broader range of environmental, climatic, and urban design variables are encouraged to refine and enhance the spatial targeting of intervention efforts.

4.7. Chapter 4 Summary

In this chapter, several spatial, temporal, and statistical analyses are introduced for a better understanding of the urban heat dynamic in Tehran city, with the help of indicators, like Normalized Difference Vegetation Index (NDVI), Land Surface Temperature (LST), and Urban Heat Island (UHI) intensity. The aim of this chapter is to identify patterns and trends to choose critical points for potential climate-sensitive areas and apply greenery-mitigation strategies.

The land cover classification between 2017 and 2023 shows a reduction in vegetated areas, especially in central and southern parts of the city, while built-up zones expanded significantly. These transformations are checked with the Difference Vegetation Index (NDVI) values, which confirm the loss of the vegetation surfaces over this time. Also, the Difference Vegetation Index (NDVI) data shows that in the areas that were already affected by extreme heat, greenery activity declined even further during the summer season.

What is more, the Land Surface Temperature (LST) analysis tells that there is evidence related to rising surface temperature, especially in areas with recent rapid urbanization, and the decadal Land Surface Temperature (LST) changes between 2014 and 2024 highlight this trend, particularly in the west, east, and south. Meanwhile, Urban Heat Island (UHI) maps help to check heat anomalies related to surrounding rural areas.

Other analysis, can be mentioned as the correlation between the Difference Vegetation Index (NDVI) and Urban Heat Island (UHI) gives a weak negative connection during mid-season and summer, which suggesting that vegetation may be help to cooling the local area, but, this correlation is positive in the winter, which may cause by the seasonal complexity of vegetation based on heat waves patterns.

At the end, for future planning, five different locations were suggested, known as critical zones for mitigation strategies. The strategy for choosing these zones is based on the overlap of low vegetation maps with high Land Surface Temperature (LST), long-term warming trends, and extreme Urban Heat Island (UHI) values. Table 18, which summarizes their spatial characteristics, environmental conditions, and general uses, also exists to support the choices of these points.

Overall, Chapter 4 has built a detailed understanding of how Tehran's urban form and surface characteristics contribute to spatial heat disparities. These findings provide an evidence-based foundation for making informed decisions about where and how to implement sustainable urban cooling measures. The next chapter will build on these insights by discussing their broader implications, addressing limitations, and outlining potential directions for future research and policy development.

5. Discussion and Conclusion

5.1. Overview of the Study

This thesis investigated Tehran's urban thermal environment through a multi-layered geospatial analysis. Utilizing satellite-derived data from Sentinel-2 and Landsat 8, the study assessed land-cover changes, vegetation dynamics (NDVI), surface temperature patterns (LST), and urban heat island (UHI) intensity across multiple years. Complementary cross-sectional profiles and pixel-level correlation analyses further clarified spatial patterns and the relationship between vegetation and surface heating. The aim was to identify high-risk thermal zones and recommend context-specific mitigation strategies, with a particular focus on vegetation-based urban cooling.

5.2. Outcomes and Explanations

The satellite images from 2017 to 2023 show urban expansion, especially in the center and south side of Tehran, which comes with a decrease in the greenery cover. Analysis of Land Surface Temperature (LST) images shows this extreme heat of these areas, but on the north side of the city, where green cover is more frequent, Land Surface Temperature (LST) is quite low compared to the other areas. The decadal analysis of the Land Surface Temperature (LST) (2024–2014) provides the spots with extreme warm weather in the west and south sides of the city.

Cross-sectional analysis confirmed the elevation effects in the Land Surface Temperature (LST) in the study area, which, in total, in low elevations, the Land Surface Temperature (LST) was higher, and vice versa. However, almost the same equal elevations in different parts of the city show different values for the Land Surface Temperature (LST), which indicates that other factors in cities, like materials and reflections of the surfaces, and greenery spaces, are still way more important for the Land Surface Temperature (LST) changes.

The correlation between Normalized Difference Vegetation Index (NDVI) and Urban Heat Island (UHI) reveals that only a modest effect from vegetation in different seasons ($R^2 \approx 0.08$), suggesting considering other urban factors like materials and reflections of the surfaces as well.

5.3. Comparison with Global Practices

Tehran's patterns align with findings in other arid and semi-arid megacities. For instance, Dubai has achieved up to 2 °C cooling in select zones by combining reflective pavements with targeted greening. Cairo's network of urban green corridors has led to significant reductions in peak temperatures, and Isfahan's revival of traditional gardens has created consistent microclimates 4–5 °C cooler than the surrounding urban fabric. These case studies (discussed in Chapter 2.5.1) highlight effective, context-sensitive solutions that Tehran could adapt, especially by leveraging culturally and climatically compatible strategies.

5.4. Implications for Urban Planning

Three main drivers underpin Tehran's rising LST and UHI:

1. **Land-use change**: The replacement of natural land covers with impervious materials significantly increases heat absorption and retention.
2. **Vegetation seasonality**: Limited and seasonal tree coverage provides only partial cooling, particularly ineffective during leaf-off periods.
3. **Surface materials**: The prevalence of dark surfaces contributes to persistent nighttime heat.

Based on these achievements, urban planners can prioritize the areas of the cities for expanding green infrastructure in thermally vulnerable zones. These green measurements can be mentioned as green roofs, green walls of the building, tree-lined streets, parks, and urban forests. Meanwhile, the utilization of reflective or lighter-color surfaces in roads and rooftops can reduce the warming effects.

5.5. Study Limitations

This study faced several constraints:

- **Temporal resolution**: using only one image per season, which may cloud cover quality, is not quite reasonable, and may not capture daily variations.
- **Spatial resolution**: Landsat-8 with a resolution of 30 m may not be quite enough for small-scale urban analysis, especially for suggesting the areas for mitigation strategies based on extreme heat.
- **Data availability**: Access to official meteorological data from the government was limited, which may have made the analysis more powerful by checking other factors, like daily precipitation, humidity, wind data, and temperature of the stations.

These limitations and other factors may have led to an underestimation of urban thermal stress and other indicators in this research.

5.6. Recommendations for Future Research

To build upon these findings, future research should:

- Utilize multi-temporal, high-frequency imagery to characterize seasonal and diurnal thermal variability more accurately.
- Utilize the new and higher resolution data from new generation satellites or sensors, and combining them with high-quality drone pictures

- Use the different factors in the analysis, like surface albedo, building height, building geometry, and wind flow in the models
- Examine socio-demographic vulnerabilities to assess the human impact of urban heat and prioritize areas for equitable intervention.
- Comparison of Nighttime and Daytime Urban Heat Island (UHI) Intensity Patterns

5.7. Conclusion

In conclusion, this research focuses on the evolution of the urban landscape in Tehran over the past decade and how these changes can influence or affect the dynamics of the land surface temperature and Urban Heat Island intensity as well. By employing satellite images data between 2014 and 2024, in this study, differences in elevations, land cover, and use transitions, the Normalized Difference Vegetation Index (NDVI), Land Surface Temperature (LST), and Urban Heat Island (UHI) patterns all around the megacity, Tehran, were analyzed. The results can show that the number of zones is undergoing very fast urban progress and expanding, especially in the west, south, and center sides of the city, even in fringe zones as well, have experienced notable warming. Checking the elevation differences in Tehran and how it can have a relationship with the Urban Heat Island and temperature fluctuation with the help of cross-section analysis shows that, most of the time, higher elevation zones experienced lower UHI and vice versa. Also, greenery land covers tell some probability to decrease the land surface temperatures, more during the mid-season and summer; still, the statistical correlation between the Urban Heat Island intensity and the Normalized Difference Vegetation Index is not so strong, and in winter season, the zones that covers with more vegetation once in a while are hotter comparison to their buildup districts around, can offer that greenery cover and zones alone cannot be enough for measuring or mitigating the Urban Heat Island fluctuation during the years. It can be said, in spite of these constraints, that vegetation covers still play an important role when it comes to the concept of climate-responsive programming, in combination with other mitigation strategies. As mentioned in previous chapters, comparison with other similar arid cities, such as Isfahan, Dubai, and Cairo, shows that it would be more effective a green infrastructure coming with other methods including reflective materials, high-albedo surfaces, and strategic land-use planning would be more effective in achieving better results of mitigating the Urban Heat Island intensity. Similar strategies could yield meaningful thermal relief in Tehran, especially in the high-risk districts identified in Chapter 4.

This research also acknowledges key limitations, including reliance on medium-resolution, single-date satellite imagery and limited access to complementary meteorological and urban data. Future studies are encouraged to build upon this foundation by incorporating higher-resolution, multi-temporal datasets and integrating additional climatic and socio-urban variables such as wind flow, albedo, humidity, and population vulnerability.

All in all, the research helps in better understanding the spatial dynamics of the Urban Heat Island dynamics in the city of Tehran and suggests a few zones for applying greenery mitigation strategies. With the help of professional planning and data-driven interventions, Tehran can progress, especially toward a sustainable city, becoming more livable, cleaner, cooler, and more climate-resilient city.

6. References

Adinna, E., Christian, E. I., & Okolie, A. T. (2009). Assessment of urban heat island and possible adaptations in Enugu urban using Landsat-ETM. *Journal of Geography and Regional Planning*, *2*(2), 030-036.

Akbari, H., Bretz, S., Kurn, D., & Hanford, J. (1997). Peak power and cooling energy savings of high-albedo roofs. *Energy and Buildings*, *25*(2), 117-123.

Akbari, H., & et al. (2001). Shade trees: Benefits and implementation challenges. *Building Research Journal*, 91-102.

Akbari, H., & Kolokotsa, D. (2016). Three decades of urban heat islands and mitigation technologies research. *Energy and Buildings*, *133*, 834-842. https://doi.org/https://doi.org/10.1016/j.enbuild.2016.09.067

Akbari, H., Menon, S., & Rosenfeld, A. (2009). Global cooling: increasing world-wide urban albedos to offset CO2. *Climatic change*, *94*(3), 275-286.

Akbari, H., Pomerantz, M., & Taha, H. (2001a). Adapted from Akbari, Pomerantz, Taha, 2001. *Energy Policy*, 295.

Akbari, H., Pomerantz, M., & Taha, H. (2001b). Cool surfaces and shade trees to reduce energy use and improve air quality in urban areas. *Solar energy*, *70*(3), 295-310.

Akbari, H., Pomerantz, M., & Taha, H. (2001c). Cool surfaces and shade trees to reduce energy use and improve air quality in urban areas. *Energy Policy*, 47-63.

Akbari, H., Pomerantz, M., & Taha, H. (2001d). Cool surfaces and shade trees to reduce energy use and improve air quality in urban areas. *Energy Policy*, *29*(6), 47-63.

Akbari, H., Pomerantz, M., & Taha, H. (2001e). Cool surfaces and urban trees as heat island mitigation measures. *Energy and Buildings*, 47-63.

Akbari, H., Pomerantz, M., & Taha, H. (2001f). Tree maintenance costs and their offset by energy savings. *Environmental Economics Journal*, 73-84.

Akbari, H., & Rose, L. (2001a). Energy Efficiency and Sustainability of Urban Heat Island Mitigation Strategies. *Journal of Urban Climate*, *17*(2), 220-240.

Akbari, H., & Rose, L. (2001b). Reflective Roofing for Urban Heat Island Mitigation. *Journal of Environmental Management*, 301-314.

Ali-Taleshi, M. S., Moeinaddini, M., Bakhtiari, A. R., Feiznia, S., Squizzato, S., & Bourliva, A. (2021). A one-year monitoring of spatiotemporal variations of PM2. 5-bound PAHs in Tehran, Iran: source apportionment, local and regional sources origins and source-specific cancer risk assessment. *Environmental Pollution*, *274*, 115883.

Alijani, B. (2004). Climatic Trends and Impacts in Iran: An Analysis of Temperature and Precipitation. *Journal of Iranian Climate Studies*, *22*(3), 320-333.

Almeida, C. R. d., Teodoro, A. C., & Gonçalves, A. (2021). Study of the urban heat island (UHI) using remote sensing data/techniques: A systematic review. *Environments*, *8*(10), 105.

Benaomar, A., & Outzourhit, M. (2024). Reforestation and Green Corridors in Cairo: A GIS Approach. *Urban Ecology Journal*, 45-60.

Berdahl, P., & Bretz, S. E. (2002). Dirt accumulation on solar reflective surfaces and its effect on the albedo. *Solar Energy Materials & Solar Cells*, *79*(2), 221-231.

Bokaie, M., Zarkesh, M. K., Arasteh, P. D., & Hosseini, A. (2016). Assessment of urban heat island based on the relationship between land surface temperature and land use/land cover in Tehran. *Sustainable Cities and Society*, *23*, 94-104.

Bretz, S. E., & Akbari, H. (1994). Performance of high-albedo materials for reducing solar heat gains in buildings. *Energy and Buildings*, *20*(1), 85-95.

Bretz, S. E., & Akbari, H. (1997). Durability and dirt resistance of high-albedo roofing materials. *Energy and Buildings*, *25*(4), 63-70.

Bretz, S. E., & Akbari, H. (1998). Potential cooling energy savings from light-colored roofs. *Building and Environment*, *33*(5), 39-56.

Busato, F., Lazzarin, R. M., & Noro, M. (2014). Three years of study of the Urban Heat Island in Padua: Experimental results. *Sustainable Cities and Society*, *10*, 251-258.

Copernicus Data Space Ecosystem Browser. (2024). https://browser.dataspace.copernicus.eu/

Corburn, J. (2007). Reconnecting with our roots: American urban planning and public health in the twenty-first century. *Urban affairs review*, *42*(5), 688-713.

Dimoudi, A., & Nikolopoulou, M. (2003). Vegetation in urban environments: Microclimatic analysis and benefits. *Building and Environment*, 383-392.

Druckenmiller, H. (2023). Urban Heat Islands 101. *Resources for the Future*. *March*, *14*, 2023.

Earth Resources, O., & Science, C. (2020a). *Landsat 8-9 Operational Land Imager / Thermal Infrared Sensor Level-2, Collection 2* (U.S. Geological Survey. https://doi.org/10.5066/P9OGBGM6

Earth Resources, O., & Science, C. (2020b). *Landsat 8 Operational Land Imager / Thermal Infrared Sensor Level-1, Collection 2* (U.S. Geological Survey. https://doi.org/10.5066/P975CC9B

Esri. (2023). ESRI Land Cover Explorer. https://livingatlas.arcgis.com/landcoverexplorer/

Fallmann, J., Forkel, R., & Emeis, S. (2016). Secondary effects of urban heat island mitigation measures on air quality. *Atmospheric environment*, *125*, 199-211.

Getter, K., & et al. (2006). Green Facades and Green Roofs in Urban Environments: A Review of the Environmental Impacts. *Urban Sustainability Journal*, 45-67.

Getter, K. L. (2006a). Energy Efficiency and Cooling Benefits of Green Roofs. *Energy and Buildings Journal*, 45-55.

Getter, K. L. (2006b). The Role of Green Roofs in Reducing Urban Heat. *Building Energy Efficiency Review*, 212-220.

Ghorbani, S. (2021). *Reduction of Urban Heat Island effects in the dry climate of Tehran, Iran*

Haghparast, A., & et al. (2020). Urban Heat Island Analysis in Tehran: Climate Adaptation and Challenges. *Urban Climate*, *12*, 45-60.

Heisler, G. M. (1989). Tree planting and cooling breezes in urban spaces. *Journal of Arboriculture*, 209-215.

Hossieni, M., & Akbari, H. (2015). The Role of Urban Surfaces in Mitigating Heat: A Case Study in Tehran. *Journal of Urban Climate*, 210-225.

Hourcade, B., & Habibi, M. (2005). Atlas de Téhéran métropole-Atlas of Tehran metropolis-Atlas kalanshahr Tehran. In: Iran;: Tehran Geographic Information Center, Municioality of Tehran.; Paris ....

Howard, L. (1833). *The climate of London: deduced from meteorological observations made in the metropolis and at various places around it* (Vol. 3). Harvey and Darton, J. and A. Arch, Longman, Hatchard, S. Highley [and] R. Hunter.

Hoyano, A. (1988). Effects of Urban Vegetation on Microclimates in Tokyo. *Environmental Research*, 150-163.

Iran Meteorological, O. (2020). Tehran climate data summary. http://www.irimo.ir

Jahadi Toroghi, F. (2005). Regional Climate Variations and Temperature Trends in Iran: A Statistical Approach. *Iranian Meteorological Journal*, *18*(4), 442-457.

Koc, S., & Güler, M. (2021). Integrating Persian Gardens into Modern UHI Mitigation Strategies: Cultural and Climatic Perspectives. *Journal of Urban Design*, *27*(4), 215-227.

Kolokotroni, M., & Giridharan, R. (2008). Urban heat island intensity in London: An investigation of the impact of physical characteristics on changes in outdoor air temperature during summer. *Solar energy*, *82*(11), 986-998.

Konopacki, S., & Akbari, H. (1997). Energy savings in buildings using reflective roofs. *Building and Environment*, *32*(4), 43-52.

Levinson, R., & Akbari, H. (2002a). Effects of albedo and emissivity on building cooling energy use in sunny climates. *Solar energy*, 49-62.

Levinson, R., & Akbari, H. (2002b). Observed performance of reflective roofs and pavements under various conditions. *Solar energy*, 74-91.

Moghbel, M., & Shamsipour, A. (2019). Spatiotemporal characteristics of urban land surface temperature and UHI formation: a case study of Tehran, Iran. *Theoretical and applied climatology*, *137*, 2463-2476.

Moisa, M. B., Gabissa, B. T., Hinkosa, L. B., Dejene, I. N., & Gemeda, D. O. (2022). Analysis of land surface temperature using Geospatial technologies in Gida Kiremu, Limu, and Amuru District, Western Ethiopia. *Artificial Intelligence in Agriculture*, *6*, 90-99. https://doi.org/https://doi.org/10.1016/j.aiia.2022.06.002

Multiple, A. (2019). Effects of prediction accuracy of the proportion of vegetation cover. https://www.sciencedirect.com/science/article/pii/S030324341930618X

Myint, S. W., Wentz, E. A., Brazel, A. J., & Quattrochi, D. A. (2021). The Use of Land Cover Indices for Rapid Surface Urban Heat Island Mapping and Monitoring. *ISPRS International Journal of Geo-Information*, *10*(6), 416. https://doi.org/10.3390/ijgi10060416

Nasehi, S., & Imanpour namin, A. (2020). Assessment of urban green space fragmentation using landscape metrics (case study: district 2, Tehran city). *Modeling Earth Systems and Environment*, *6*(4), 2405-2414.

Niachou, K., & et al. (2001). Effect of Urban Green Spaces on Air Quality in Metropolitan Areas. *Environmental Management*, 128-136.

Nuruzzaman, M. (2015). Urban heat island: causes, effects and mitigation measures-a review. *International Journal of Environmental Monitoring and Analysis*, *3*(2), 67-73.

Oke, T., & Cleugh, H. (1987). The Impact of Urban Surfaces on Climate. *Journal of Climate Studies*, 45-52.

Oke, T. R. (1982). The energetic basis of the urban heat island. *Quarterly journal of the royal meteorological society*, *108*(455), 1-24.

Pearlmutter, D., & et al. (2009). Effects of green vegetation on air quality in urban areas. *Journal of Environment and Ecology*, 89-100.

Rahimzadeh, F., & Asgari, M. (2007a). Climatic Trends in Iran: Temperature and Precipitation Analysis from 1951 to 1997. *Iranian Climate Change Journal*, *25*(3), 78-95.

Rahimzadeh, F., & Asgari, M. (2007b). Long-Term Climatic Data Analysis in Iran: A Study of 27 Synoptic Stations. *Journal of Meteorology*, *36*(2), 188-202.

Rasooli, F. (2006). Temperature Trends and Precipitation Variability in Iran: A Decade of Climate Change Studies. *Geographical Research*, *14*(2), 120-136.

Razzaghmanesh, M., & Beecham, S. (2018). A review of permeable pavement clogging investigations and recommended maintenance regimes. *Water*, *10*(3), 337.

Razzaghmanesh, M., Borst, M., Liu, J., Ahmed, F., O'Connor, T., & Selvakumar, A. (2021). Air temperature reductions at the base of tree canopies. *Journal of sustainable water in the built environment*, *7*(3), 04021010.

Razzaghmanesh, M., & et al. (2018a). GIS-based UHI Analysis and Mapping in Tehran: A Tool for Urban Planning and Intervention. *Urban Climate Studies*, *24*(4), 110-125.

Razzaghmanesh, M., & et al. (2018b). Spatial Analysis of Urban Heat Islands Using GIS: A Case Study of Tehran. *Urban Climate Research Journal*, 99-114.

Robitu, M., & et al. (2006a). Evaporative cooling effects of urban water bodies. *Urban Climate Journal*, 28-35.

Robitu, M., & et al. (2006b). The role of urban parks in local temperature reduction. *Urban Studies*, 1181-1197.

Robitu, M., & et al. (2006c). Thermal properties of urban water bodies and their impact on local temperatures. *Environmental Science and Urban Planning Review*, 52-60.

Rosenfeld, A. H., & et al. (1992). Mitigation of Urban Heat Islands: Materials, Utility Programs, and Updates. *Atmospheric environment*, *25B*(6), 100-112.

Roth, M. (2009). Effects of cities on the local climate and the relationship with climate change mitigation and adaptation. IOP Conference Series. Earth and Environmental Science,

Sailor, D. (2002). Urban heat islands, opportunities and challenges for mitigation and adaptation. *Sample Electric Load Data for New Orleans, LA (NOPSI, 1995). North American Urban Heat Island Summit. Toronto, Canada*, 1-4.

Sailor, D. (2006). Reflective and Permeable Pavements for UHI Mitigation. *Journal of Urban Climate*, 34-46.

Sailor, D. J. (2006a). Climate resilience and the role of vegetation. *Journal of Urban Climate*, 400-412.

Sailor, D. J. (2006b). *Urban Heat Island Mitigation: Research, Strategies, and Solutions*. Cambridge University Press.

Sailor, D. J. (2006c). *Urban Heat Island Mitigation: Research, Strategies, and Solutions*. Cambridge University Press.

Sailor, D. J. (2006d). Urban Heat Islands: Strategies for Mitigation. *Urban Climate Research Review*, 389-404.

Sailor, D. J. (2006e). Urban Heat Islands: Strategies for Mitigation. *Urban Climate Research Review*, 390-405.

Sailor, D. J. (2006f). Water infiltration and cooling: Impacts on urban temperature. *Urban Climate Journal*, 412-421.

Santamouris, M., Ding, L., Fiorito, F., Oldfield, P., Osmond, P., Paolini, R., Prasad, D., & Synnefa, A. (2017). Passive and active cooling for the outdoor built environment–Analysis and assessment of the cooling potential of mitigation technologies using performance data from 220 large scale projects. *Solar energy*, *154*, 14-33.

Santamouris, M., & et al. (2012a). The Effectiveness of Cool Roofs for Mitigating Urban Heat Island. *Environmental Engineering and Management*, 123-136.

Santamouris, M., & et al. (2012b). Urban Heat Island Mitigation Strategies: Integrating Green and Built Solutions in Modern Cities. *Environmental Management and Urban Sustainability*, *5*(3), 85-98.

Scott, K., Simpson, J., & McPherson, G. (1999). Impact of urban tree-planting programs on energy savings and air quality improvement. *Urban Forestry Journal*, 12-19.

Sodoudi, S., Shahmohamadi, P., Vollack, K., Cubasch, U., & Che-Ani, A. (2014). Mitigating the urban heat island effect in megacity Tehran. *Advances in Meteorology*, *2014*(1), 547974.

Statistical Center of, I. (2022). *Iran Statistical Yearbook 2021–2022 (1399)*. https://www.amar.org.ir/en/Statistics-by-Topic/Environment-and-multi-domain-statistics/Yearbooks-and-similar-compendia/Yearbook#4990353-iran-statistocal-yearbook-2021-2022-1399

Statistical Centre of, I. (2016). *Iran Population and Housing Census 2016*. http://www.amar.org.ir/english

Steenveld, G. J., & Heusinkveld, B. G. (2012). Urban climate research with portable instrumentation. *Journal of Urban Climate*, 57-72.

Survey, U. S. G. (2017). NDVI, the Foundation for Remote Sensing Phenology. https://www.usgs.gov/special-topics/remote-sensing-phenology/science/ndvi-foundation-remote-sensing-phenology

Survey, U. S. G. (2021a). How do I rescale Landsat Level-1 digital numbers to reflectance, radiance, and brightness temperature? https://www.usgs.gov/faqs/how-do-i-rescale-landsat-level-1-digital-numbers-reflectance-radiance-and-brightness

Survey, U. S. G. (2021b). Landsat Normalized Difference Vegetation Index. https://www.usgs.gov/landsat-missions/landsat-normalized-difference-vegetation-index

Survey, U. S. G. (2021c). Using the USGS Landsat Level-1 Data Product. https://www.usgs.gov/landsat-missions/using-usgs-landsat-level-1-data-product

Synnefa, A., Santamouris, M., & Livada, I. (2008). A review of the thermal performance of reflective materials. *Journal of Urban Environment*, 160-174.

Tabrizian, M., & et al. (2021). Challenges in UHI Spatial Analysis in Tehran: Data Gaps and Solutions. *International Journal of Urban Climate*, *29*(3), 50-67.

Tagavi, M., & Mohammadi, A. (2012). Cold and Warm Events in Iran: Climate Change Patterns. *Meteorological Research*, *29*(6), 462-475.

Taha, H. (1997). Mitigating Urban Heat Island Effects in the Tropics: The Role of Cool Roofs. *Environmental Research*, 97-106.

Taha, H., & Rainer, L. (1997). Holistic Approaches to Urban Heat Island Mitigation: Integrating Green Infrastructure and Advanced Materials. *Journal of Environmental Studies*, *12*(1), 34-42.

Talkhabi, H., Jafarpour Ghalehteimouri, K., & Toulabi Nejad, M. (2024). Integrating Tehran metropolitan air pollution into the current transport system and sprawl growth: an emphasis on urban performance and accessibility. *Discover Cities*, *1*(1), 6.

Theuwes, A., & et al. (2014). The Impact of Water Bodies on Urban Heat Island Effect: A Case Study in Rotterdam. *Environmental Science and Technology*, 78-82.

Theuwes, N., & et al. (2012). Impact of thermal inertia on urban night cooling. *Building Research Review*, 53-67.

Theuwes, N. E., & et al. (2012). Measuring urban climate using portable instruments. *Urban Climate*, 57-72.

Un-Habitat. (2008). *State of the World's Cities 2008/9: Harmonious Cities*. Earthscan.

USGS EarthExplorer. (2025). https://earthexplorer.usgs.gov/

Vafa, A., & Kiani, B. (2020). Green Roofs as a Strategy to Combat Urban Heat Island Effects in Tehran: A Case Study. *Urban Environmental Journal*, 112-120.

Voogt, J. A. (2004). Urban heat islands: hotter cities. *American Institute of Biological Sciences*.

Wilmers, F. (1988). Effects of vegetation on urban climate and air quality. *Atmospheric environment*, 251-267.

Wong, N. H. (2005). Green Roofs for Urban Heat Island Mitigation. *Urban Environmental Management Journal*, 129-135.

Yamamoto, R. (2006). Urban Planning Strategies for Cities Near Rivers. *Environmental Planning Journal*, 34-48.

Yao, Y., & et al. (2024a). GIS-Based Urban Heat Island Mitigation in Dubai. *Journal of Environmental Management*, 122-135.

Yao, Y., & et al. (2024b). Integrating Traditional Urban Design and Modern Solutions: A Case Study of Isfahan. *Urban Design Review*, 200-215.

Zahrani, H. (2013). Urban Heat Island Effects and Urbanization: A Case Study in Iran's Semiarid Regions. *Journal of Environmental Planning*, *31*(1), 102-115.

Zarei, S., & Tagavi, M. (2010). Warming Trends in Iran's Coastal Areas: Implications for Climate Adaptation. *International Journal of Climate Science*, *12*(2), 314-322.

Zargari, M., Mofidi, A., Entezari, A., & Baaghideh, M. (2025). Climatology of Tehran surface heat Island: a satellite-based spatial analysis. *Scientific Reports*, *15*(1), 10567.

Zawar-Reza, P. (2008). Numerical Analysis of the'120 Day Wind'over the Sistan Region, South-West Asia with TAPM. *Clean Air and Environmental Quality*, *42*(1), 21-24.

Zhao, L., & et al. (2014). Use of Remote Sensing Data for Monitoring Urban Heat Island Effects in Tehran. *Journal of Environmental Science*, 231-245.

Zhao, W., & et al. (2014). Long-term Effects of UHI Mitigation in Arid Regions: Case Studies and Challenges. *Environmental Impact Assessment Review*, *44*, 30-40.